Diploma Thesis

Evaluation of N_2O emissions of MABR treating SDE

by Markus Latschbacher

Supervisor:
Ass.Prof.Dr.techn. **Svardal** Karl
Dipl.-Ing. Dr.techn **Parravicini** Vanessa

Technische Universität Wien
Institute for Water Quality, Resources and Waste Management

Vienna, Mai 2017

I want to thank everybody for their support who made my graduation possible, especially my family and those I love.
I want to thank Mrs. Daniela Reif and all my other colleges who supported me during the sometimes exhausting but mostly delightful time at TU Wien.
Further, I want to thank the Institute for Water Quality, Mr. Jörg Krampe and Mr. Karl Svardal for the interesting topic and their support and, above all, I want to thank Mrs. Vanessa Parravicini for the outstanding mentoring for this thesis.

This work is dedicated to Maria Magdalena Rosenberger,

Danke!

Abstract

Anaerobic digestion is commonly used on bigger wastewater treatment plants to transform organic matters of surplus activated sludge into biogas to gain energy. The effluent from this anaerobe digestion is dewatering which results in a highly ammonium loaded effluent called sludge dewatering effluent (SDE). It is said, that the amount of ammonium in SDE contributes up to 25% of the nitrogen load of a wastewater treatment plant (Meyer et al., 2004). The emission of the greenhouse gas nitrous oxide (N_2O) at wastewater treatment plants is gaining attention over the last years. N_2O is a byproduct in the process of converting ammonium to nitrite (nitritation) and denitrification, therefore the treating of highly ammonium loaded wastewater such as SDE has a high potential for emitting N_2O. A new concept for treating SDE in the side stream before recycling the stream into the main stream basin was introduced, which leads to a reduction of the energy costs for aeration (Krampe et al., 2016). One possible way to achieve nitritation of SDE in side stream is a membrane aerated biofilm reactor (MABR), which is investigated in this thesis. Therefore, SDE from a municipal wastewater treatment plant was treated over 98 days in a lab scale MABR, focusing on the ammonium removal rate, the nitritation rate as well as the N_2O emissions during the process. At the end of the process time an ammonium removal rate of 12.8gNH_4-N/m²/d was achieved while the N_2O emissions of the plant was 1.7%N_2O-N/ NH_4-N_{conv}.

1 Introduction

By anaerobic digestion organic matters of surplus activated sludge is partially transformed into biogas with 60 – 70vol% methane CH_4 (Appels et al., 2008). The energetic use of biogas to produce electric energy or heat is common at large wastewater treatment plants (WWTP) and represents an effective way to produce renewable energy (Chen, et al., 2015). After the anaerobic digestion, the sludge is dewatered to reduce the costs for transportation and disposal. The resulting sludge dewatering effluent (SDE) is highly loaded with ammonium (500 – 1,500mg NH4-N/L) (Wang, et al., 2014) and requires further treatment.

It is common practice to bring the SDE back into the activated sludge basin in mainstream where ammonium is converted to nitrate by nitrifying bacteria. An innovative treatment concept for SDE targets the nitritation (partial oxidation of ammonium to nitrite) in the side-stream prior recycling the treated stream into an anoxic part of the mainstream basin (Krampe et al., 2016). The concept provides a significant reduction of energy for aeration especially at two stage WWTPs. However, one drawback of nitritation in SDE is the intensive production and emission of the greenhouse gas nitrous oxide (N_2O).

By the biological oxidation of NH_4-N to nitrite, N_2O is produced as byproduct and dissolves in the liquid phase. Parts of the dissolved N_2O is stripped out of the activated sludge basin during aeration for nitrification and comes into the atmosphere. The production and emission of N_2O by SDE sidestream nitritation is known to be higher than in mainstream nitrifying basins, mainly due to the high ammonium and nitrite concentrations and low levels of dissolved oxygen (DO) applied (Pijuan et al., 2014). It is said, that 7,442kt CO_2 equivalents of N_2O were emitted by the EU 28 in 2014 from wastewater handling, which is about 0.2% of the total emitted greenhouse gases of 2014 (UNFCCC, 2016).
The attention that N_2O emissions are receiving at WWTPs is increasing. Due to the fact, that it is the third largest greenhouse gas (after carbon dioxide and methane) and has a global warming potential 298 times stronger than CO_2 (IPCC, 2007), its emission should be reduced wherever possible.
A membrane aerated biofilm reactor (MABR) can provide some major benefits. By using membranes for oxygen transfer over a gas-transfer membrane, aeration with low energy input for nitrification can be provided. Oxygen is transferred without bubbles through the gas-transfer membrane, which favors the establishment of a nitrifying biofilm. It is said, that an aeration efficiency of 6kg O_2/kWh can be achieved with MABR technology (Côté et al., 2015). The bacteria on the biofilm use the provided oxygen, whereby the DO in the liquid phase is zero, which indicates very efficient use of oxygen. Additionally, due to the lacking of air bubbles, the transfer of N_2O from the liquid to the air can be reduced compared to conventional bubble aeration.

The MABR technology was applied to treat a synthetic ammonium solution (Adams et al., 2014) as well as sewage primary effluent in pilot scale (Cote et al., 2015) but never for treating SDE in side stream. The treated SDE can then be brought into an anoxic part of a WWTP, whereby the energy costs as well as the N_2O emission can be reduced compared to conventional treatment of SDE. In addition, the N_2O that counter diffuses from the bulk into the membrane chords and leaves the MABR with the process air can be further treated before releasing it into the atmosphere.

The goal of this study is to assess the suitability of the MABR technology to treat SDE at lab-scale and in particular 1) to ascertain the maximum process performance at set process air 2) to investigate the possibility to gain stable partial nitrification and 3) to estimate the reduction potential on N_2O emission from the nitritation process.

2 Theoretical Background

The removal of nitrogen is a crucial part of municipal wastewater treatment; therefore, nitrification plays a major role. The stoichiometric reaction of the oxidation of ammonium to nitrite via nitrification is described in Eq.1, the further oxidation to nitrate is described in Eq.2 According to today's state of knowledge, these reactions are performed by Nitrosomonas and Nitrobacter which are both autotrophic bacteria (Sinha and Annachhatre, 2006). Anyway, many different microorganism take part in wastewater treatment plants, so the bacteria that perform the reaction described in Eq.1 are called ammonium oxidizing bacteria (AOB) while the ones for Eq.2 are called nitrite oxidizing bacteria (NOB). Acid is formed and alkalinity is consumed during nitritation (Eq.1), therefore the pH will decrease with higher nitritation degree.

$$NH_4^+ + 1.5O_2 \rightarrow 2H^+ + H_2O + NO_2^- \qquad \text{Eq.1}$$

$$NO_2^- + 0.5O_2 \rightarrow NO_3^- \qquad \text{Eq.2}$$

Partial nitrification or nitritation has major benefits for treating wastewater with high ammonium loading and low carbon content such as SDE. Nitritation takes 26% less oxygen for oxidation than nitrification. Further, when brought into the anoxic part of the WWTP, the demand of C-source is reduced by 40% for denitritation (Krampe, 2016). This means that high potential of saving energy lies in this process strategy. The concept also works in a single stage WWTP, while the potential for energy savings is higher in a 2-stage WWTP. A scheme of a 2 - stage WWTP with SDE side stream treatment is shown in Figure 1.

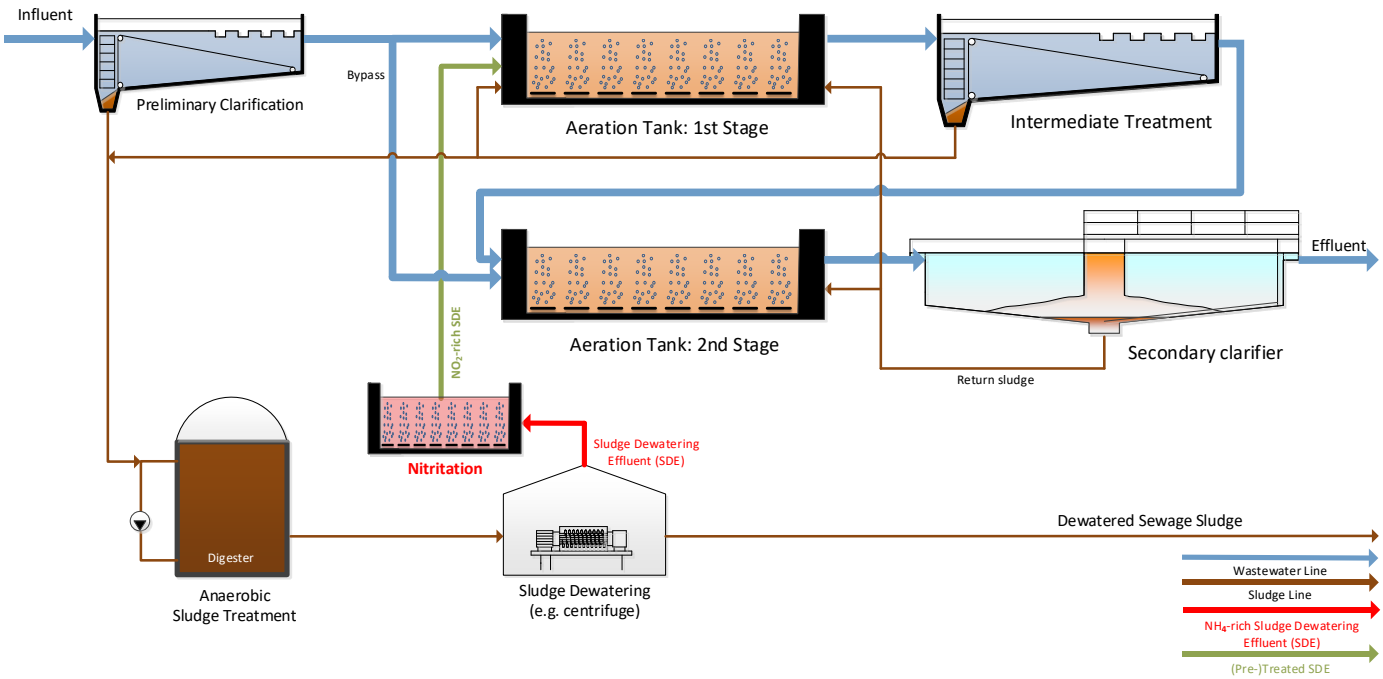

Figure 1 Scheme of a 2- stage wastewater treatment plant with MABR treatment

One way to prevent the oxidation of nitrite to nitrate would be to increase the temperature (30 – 40°C) (Hellinga, et al. 1998), another way would be to apply low solid retention time (SRT) (Lackner, et al. 2010). A different method would be to run the reactor under a condition of oxygen limitation since the oxygen affinity of AOBs is higher than for NOBs and therefore, an oxygen limitation would benefit the AOBs (Blackburne at al., 2008).

Additionally, free ammonia (FA) as well as free nitrous acid (FNA) are known to inhibit NOBs and AOBs. Ammonium (NH_4^+) is the dissociated form of free ammonia (NH_3), nitrite (NO_2^-) the dissociated form of free nitrous acid (HNO_2), the dissociation equilibrium is depending on pH value and temperature.

It is said, that FA of 0.1 – 1.0mgN/L starts to inhibit NOB (Anthonisen, 1976). At pH 8 and 4.8 mg/L initial FA a 60% nitrite accumulation was observed, while inhibition already started at 0.1 – 4.0 mg/L (Bae et al., 2001). 0.026 – 0.22mgN/L FNA can completely inhibit NOB (Zhou et al., 2010). Both tests mentioned above were performed with synthetic wastewater, which had a way higher ration of COD to NH4-N than the SDE in this study. Further the used sludge in the studies was flocculent and not a biofilm. Flocculent sludge is not as dense as a biofilm and therefore, the liquid phase can penetrate it more easily. Through that, flocculant sludge is more affected by changes in the process conditions (such as change of the pH value, etc.) than a biofilm is. In addition, adaptation of bacteria to inhibiting agents also ampers the comparison of threshold values among different research studies.

Figure 2 shows the concentration of FA with different pH values and NH_4-N concentrations, the black line indicates the threshold for inhibition of NOBs (4mg/L) for flocculent sludge according to Bae (2001). Eq. 3 was used for calculation. Figure 3 shows the concentrations of FNA with different NO_2-N concentrations while Eq. 4 was used for calculation. The black line indicates the threshold were NOB inhibition starts according to Zhou et al. (2010). Both, Eq. 3 and Eq. 4 are reported in Ge et al. (2014).

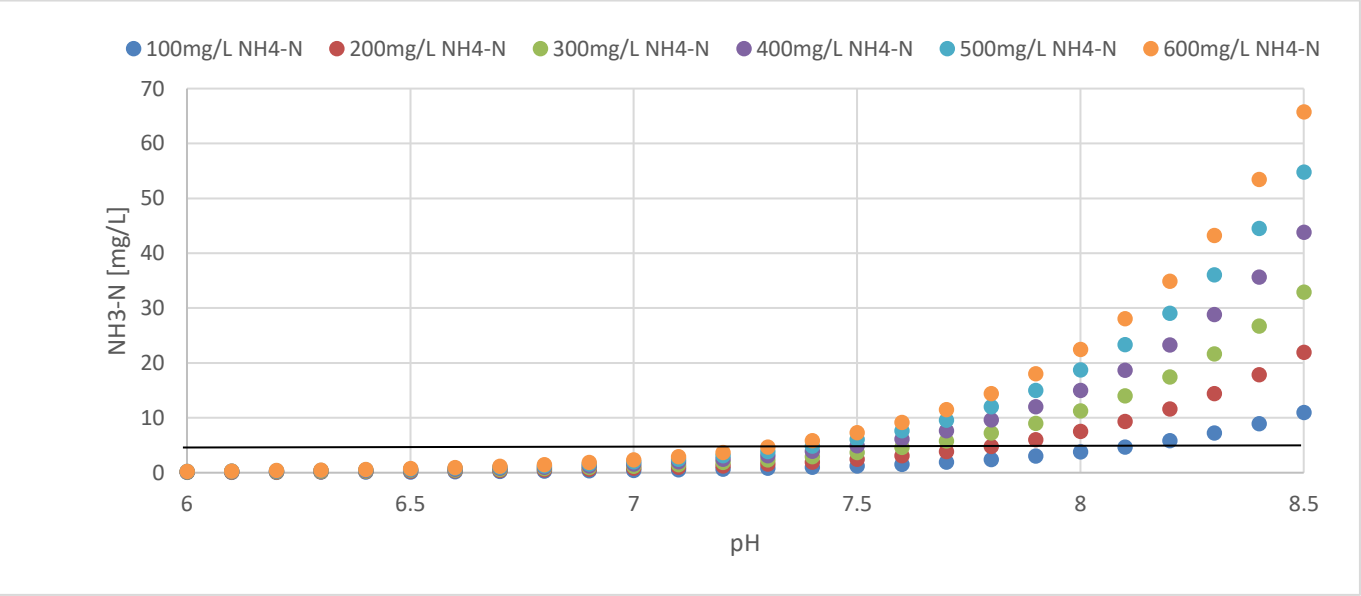

Figure 2 Concentration of free ammonia (FA) at different pH values and ammonium concentrations. Threshold values for complete inhibitions of NOBs in flocculent sludge according to Anthonisen (1976)

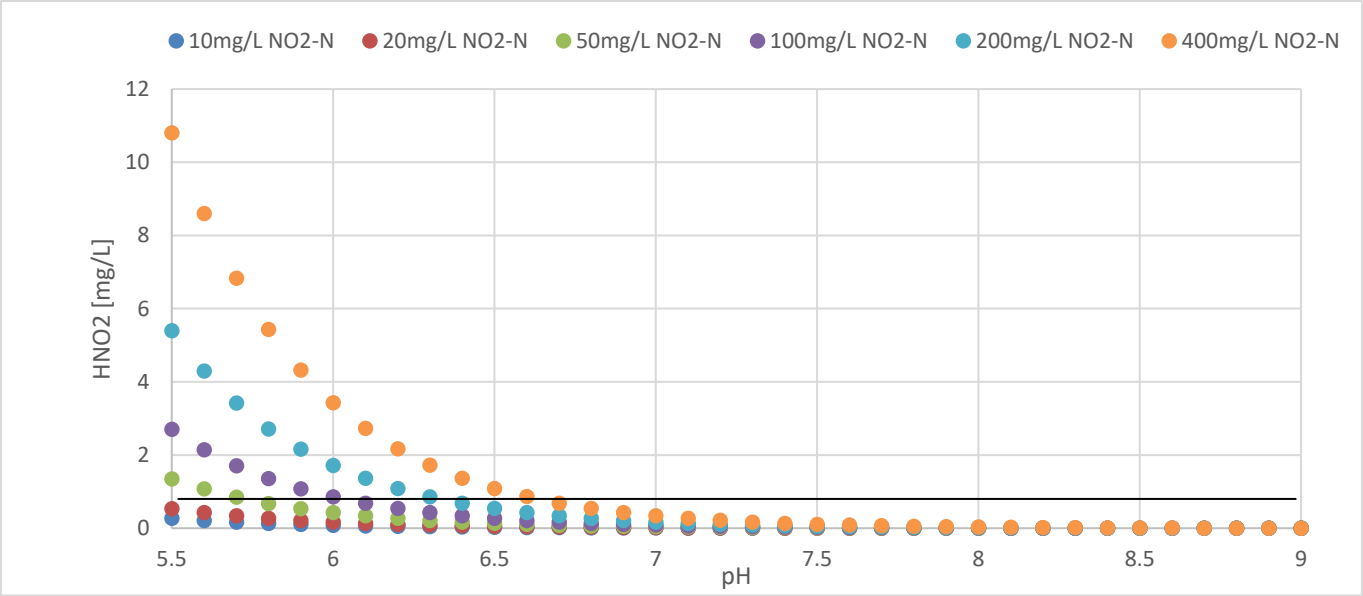

Figure 3 Concentration of free nitrous acid (FNA) at different pH values and ammonium concentrations. Threshold values for complete inhibitions of NOBs in flocculent sludge according to Zhou et al. (2010)

$$FA = \frac{17 S_{NH_4-N} * 10}{14 * (e^{\frac{6344}{273{,}15+T}} + 10^{pH})} \qquad \text{Eq.3}$$

$$FNA = \frac{47 S_{NO_2-N}}{14 * (e^{-\frac{2300}{273{,}15+T}} * 10^{pH} + 1)} \qquad \text{Eq.4}$$

FA and FNA not only inhibits NOBs but also AOBs, which should be avoided. It is said, that inhibition of AOBs starts at 40 – 200mgNH_3/L and 0.02 to 0.1mgHNO_3/L (Nowak, 1996). Like for the thresholds of NOBs, these values are neither investigated for MABR technology nor for SDE, so the values should not be taken for granted for the technology used in this thesis.

The most suitable approach to manage partial nitrification in MABR from the ones mentioned above is the low DO as well as the control of the pH value in combination with FA and FNA inhibition. Additionally, the control of the temperature could benefit the partial nitrification. SDE has a temperature of about 25°C when leaving the centrifuge, therefore a process at higher temperature would be possible easily. The control of the sludge retention time (SRT) is not possible in biofilm systems as MABR.
Due to the almost infinite SRT, several different microorganisms can grow inside the biofilm, so it can be hard to get rid of unwanted ones once they are inside the system.
One investigation regarding nitritation with MABR can be found in the literature. There, 92% partial nitrification was achieved with synthetic wastewater (200mgNH_4-N/L) and a temperature of 35°C (Gong et al., 2007). To the author's knowledge, treating SDE with MABR was investigated for the first time in this thesis.

Biological nitrogen conversion is shown in Figure 4. At the oxidation step 1 from NH_4^+ to NO_2^-, performed by AOB in the biofilm, N_2O is a byproduct. In step 6 the N_2O is converted to N_2 by heterotrophic denitrifying bacteria and can be emitted with no impact on climate change. Since SDE contains little degradable COD, denitrification is limited.

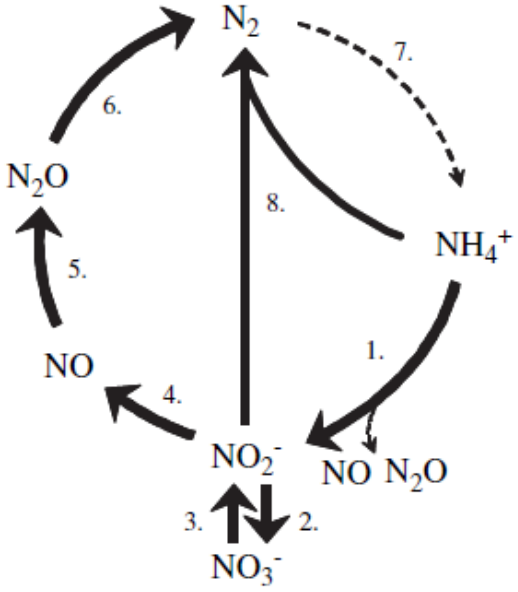

Figure 4 Biological nitrogen conversions. (1) Aerobic ammonia oxidation (autotrophic and heterotrophic AOB and AOA), (2) aerobic nitrite oxidation (NOB), (3) nitrate reduction to nitrite (DEN), (4) nitrite reduction to nitric oxide (AOB and DEN), (5) nitric oxide reduction to nitrous oxide (AOB and DEN), (6) nitrous oxide reduction to dinitrogen gas (DEN), (7) nitrogen fixation (not relevant in most WWTPs), (8) ammonium oxidation with nitrite to dinitrogen gas (Anammox). Complete nitrification comprises step 1 and 2, complete denitrification step 3–6 (Kampschreur 2009)

Several investigations concerning the production and emission of N_2O at WWTPs are reported in the literature. The variability range of N_2O emissions measured at WWTPs so far is wide. EFs expressed as kg N_2O-N emitted per influent kg TN vary between 0.003 und 2.6 % (Parravicini et al, 2015). This pronounced variability mainly derives from the significant impact that operating conditions have on N_2O production (Kampschreuer et al., 2009). In particular, high NH_4 concentration and loading rate, high NO_2^-concentration and low DO level are known to trigger the production on N_2O.

The principle of an MABR is shown in Figure 5. Air flows with low pressure (25kPa in this thesis) through oxygen permeable hollow fiber membranes, while oxygen is diffusing through the membrane surface. By the principle of the bubbleless aeration which can be achieved by MABR technology, no dissolved oxygen is in the bulk liquid. Bacteria from the bulk liquid settle on the membrane surface and form a biofilm due to the high oxygen concentration and perform the oxidation process mentioned above. In ideal all the oxygen is consumed by the biofilm, whereby the DO inside the bulk liquid is 0. Additionally, the air inside the membranes (process air) does not have to form bubbles and therefore does not need to overcome the hydrostatic pressure of the tank. Still the hydrostatic pressure of the liquid reduces the O_2 driving force over the membrane induced by the air pressure. Also, it can be assumed that the oxygen concentration inside the process air that is flowing through the membranes is decreasing from top to bottom, which again results in a decrease of the driving force due to O_2 concentration gradient.
High oxygen efficiency as well as high ammonium removal is the result of MABR. One investigation reported an NH_4-N removal rate of 3gNH_4-N/d/m² using municipal wastewater and MABR technology. Also, a maximum OTE of 0.5 – 0.55 was achieved (Cote et al., 2015). Another study reported a specific nitritation rate of 5.4 gNH_4-N/m²/d using synthetic wastewater (Brindl et al., 1998)

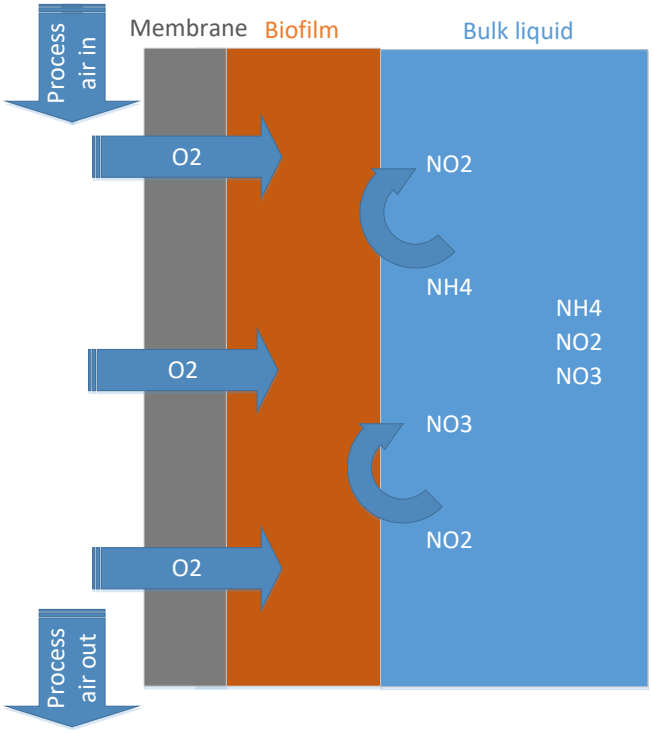

Figure 5 Function principle of nitrification in MABR

There are two points where N_2O can be emitted at MABR: 1) at the top of the module where the air streams used for mixing of the bulk liquid and for scouring of the biofilm leave the MABR and 2) the off gas of the process air. The fact that N_2O can be detected in the off gas indicates that the driving force due to different N_2O concentrations in the biofilm and in the process air is just as important as the contribution of the pressure to it.

3 Material and Methods

A lab-scale MABR was built up (Figure 6). Three membrane modules with reactor heights of 1.2m and a reactor volume of 0.72L each were used. Each module contained 10 Zeelung hollow fibre membranes (GE Power, USA) with a total surface area of 0.1m^2

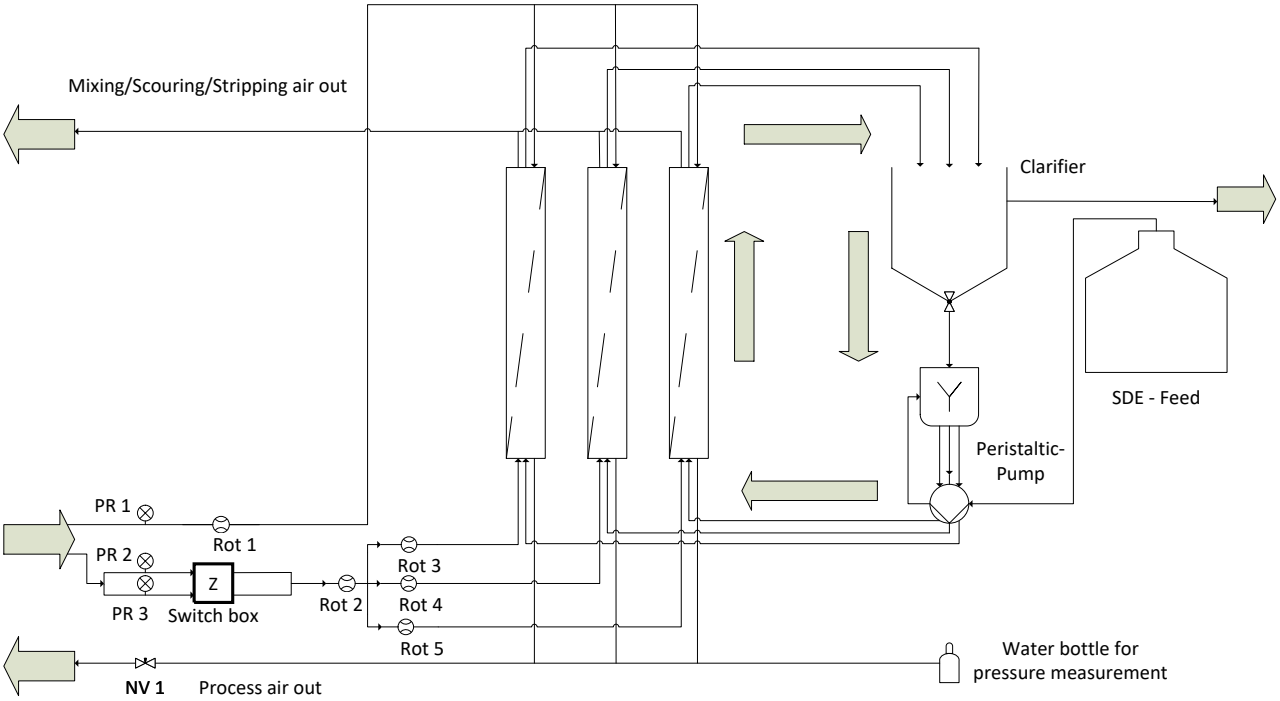

Figure 6 Flow chart of the lab scale MABR plant

As seed sludge 1L flocculent sludge from a full-scale SDE treatment plant for nitritation as well as 0.5L SDE, diluted with 2.5L water were brought into the reactor as feed during the startup. The modules were filled with tap water at the beginning of the process.

To support the growth of the biofilm on the membranes, the MABR was run as a hybrid process. A clarifier (Festo, Germany) with a volume of 3L was set after the membrane modules. The influent (SDE) was mixed with the return effluent of the clarifier in ratio 1:2 before being pumped (peristaltic pump) into the modules. In this way, the flocculent seed sludge was recirculated back and thereby held in the system. The hybrid process was operated also after the biofilm was established on the membranes

The process was run at room temperature (in average 22°C)

Figure 7 shows one single membrane module.

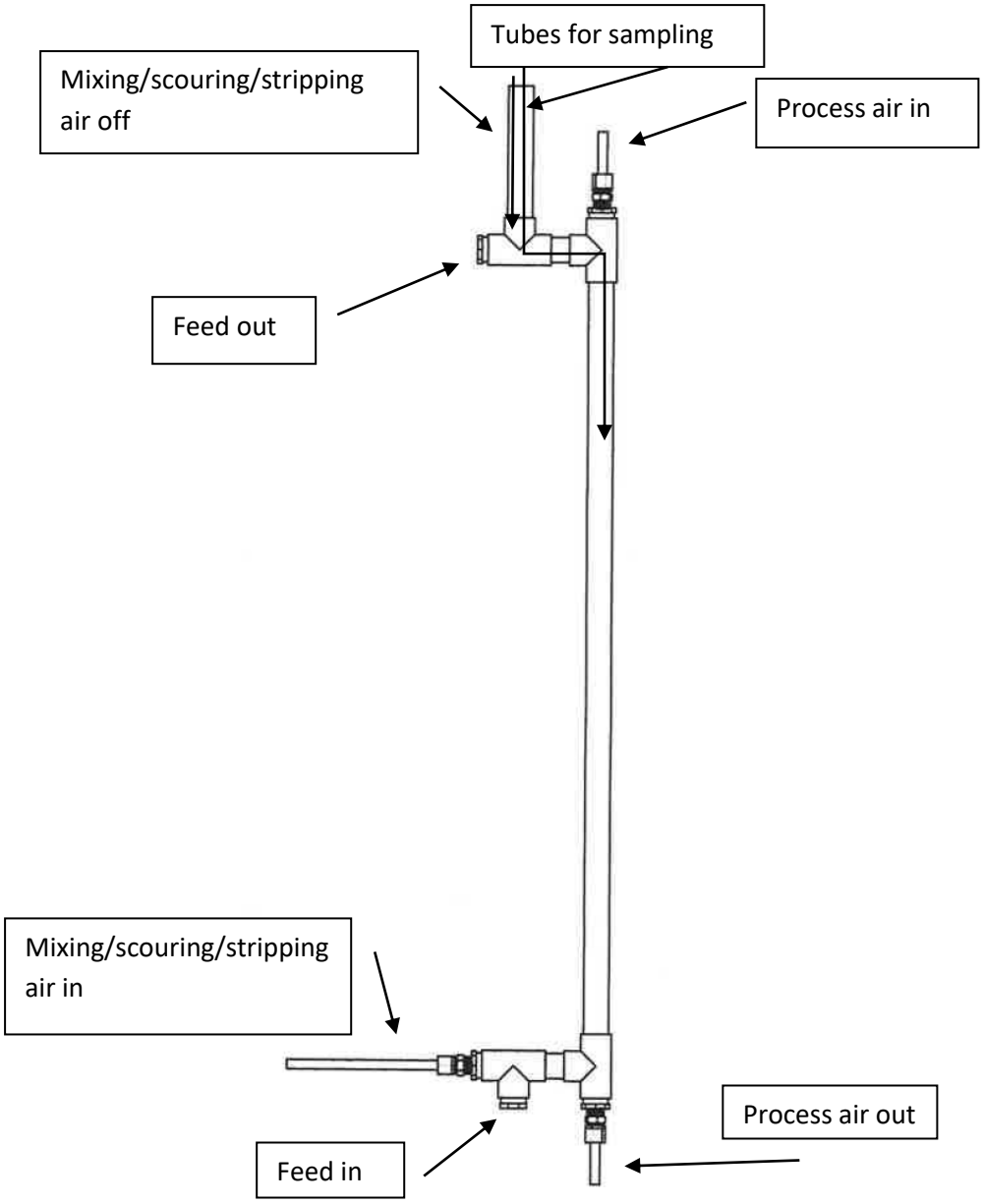

Figure 7 Sketch of a single membrane module

The fed SDE was collected at a municipal wastewater treatment plant with anaerobic digestion with a population equivalent (p.e.) of 165.000. The anaerobic sludge is dewatered at the plant using polymers and a centrifuge. New feed was taken in two week's intervals. To make analysis easier and to prevent clogging of the tubes, the SDE was sieved with an 1mm sieve.
The characteristic of the feed over the process time is shown in Table 1.

Table 1. Characteristics of feed over the process

	NH_4 –N [mg/L]	COD [mg/L]	CODmf [mg/L]	BOD [mg/L]	Suspended solid [mg/L]
SDE	1010 ±82 (n=8)	320 ±44 (n=7)	208 ±4 (n=6)	68 (n=1)	60±18 (n=6)

The lab-scale trials ran over 98 and can be split in four phases.

- Phase 1 (1-44): Development of biofilm by feeding diluted SDE
- Phase 2 (45-75): Support biofilm growth by feeding undiluted SDE with increasing NH_4-N loadings
- Phase 3 (76-88): As phase 2 with defined process air in flow (1 L/h) by targeting maximum performance of the plant
- Phase 4 (89-98): Increase of the process air in flow to 2.1 L/h to target maximum performance of the plant

During phase 1 1 L/d of SDE were mixed with 2 L/d of return flow of the clarifier ad pumped into the modules. During this first operation period the feed was diluted with water. For the rest of the rest of the operation undiluted SDE was fed at different flowrate, while keeping the ratio of SDE to recirculation at 1:2.

Before starting the operation, it was verified that the return flow from the clarifier and the fed SDE were mixed properly before being split onto each module. Proper mixing was ensured by spiral-wrapping the tube after the mixing point around a cylinder (d=3cm) (indicated as a mixer in Figure 6) and validated by tracer measurements mixing tap water from the clarifier with an NH_4-N stock solution as feed. Additionally, the influent flowrate to each module was measured.

The airflow setup of the plant is shown in (Figure 8). The bulk liquid in the modules were mixed by using coarse bubble sparging. Mixing was performed to keep the bulk liquid well mixed and was done 10 seconds on/ 110 seconds off with a flow rate of 220 mL/min for each module. The air flow rate was pre-adjusted by using Rot 2, the fine adjustments were done with Rot 3 to 5. To validate the adjustments, a water displacement column was used to measure the airflow rate. Therefore, a graduated cylinder was submerged upside down in a cylindrical water vessel while the inlet at its top was connected to the headspace of the module. By monitoring the water displacement in the graduated cylinder over the time, the air flow was measured accurately with this method.
To remove surplus biofilm or particles, a scouring was performed two times a day for three minutes with a volume of 1.35L/scouring for module A, 1.73L/scouring for module B and 1.58L/scouring for module C.
Two pressure reducers were used to adjust the pressure for mixing (PR 3) and scouring (PR 2). The intervals were controlled with a switch box.

The process air for oxygen supply of the biofilm was provided via a compressor. It was made sure, that the backpressure at the end of the membranes was at 25kPa constantly by adjusting the pressure with PR 1 as well as the flow with the needle valve NV 1. The pressure was measured by using a water bottle with a tube connected to the tube of process air out. Due to the air pressure, the water from the bottle rose in a second vertical tube, the water level difference between the bottle and the tube provided the air pressure valve (meter water column), similar as in a u tube manometer.
Surplus O_2 supply for AOBs was provided in operation phase 1 and 2, for operation phase 3 the process air at the input was set to 1L/h in total, for operation phase 4 the air was set to 2.1L/h. A leakage was detected at process day 76 at NV1, revealing, that much more process air had been conveyed into the membranes then the one expected based on measurements in process air out. After the fixing, the process air in was decreased to 1L/h, as already mentioned. Since the airflow was

higher before the fixing of the leakage, the AOBs were O_2 limited at this reduced airflow rate, and therefore the feed had to be decreased at process day 80. Then the process air in was set to 2.1L/h at process day 89 (operation phase 4) to find out about the maximum performance of the plant.
After the detection of the leakage, when the air flow was set to 1L/h, the pressure at the inlet side of the membranes (PR 1) was set to 28kPa. At process day 87, when the air flow was set to 2.1L/h the mentioned air pressure was set to 35kPa.
Air loss in form of fine bubbles released over the surface of the membranes (in the following "stripping air") was observed and measured with the water displacement method mentioned above (graduated cylinder). Stripping air was 0.17 L/h for all three modules together.
The scheme of the air flows with the nomenclature is shown in Figure 8.

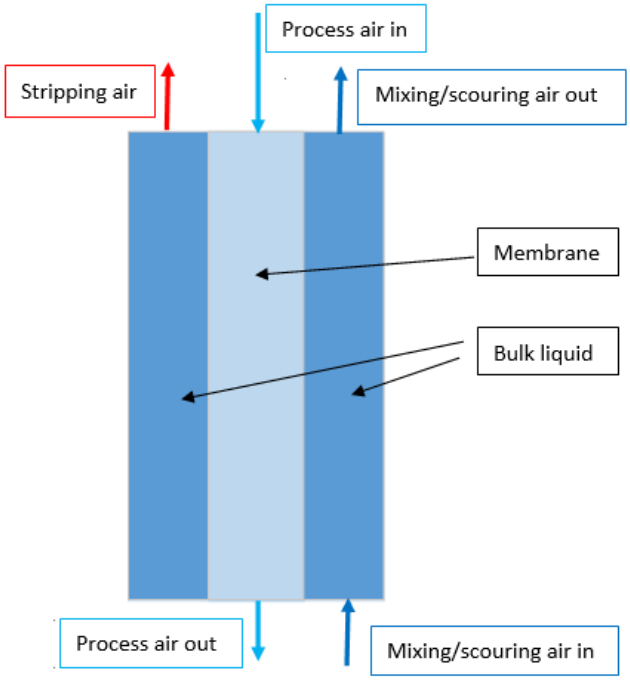

Figure 8 Naming of the air flows

Liquid samples for analyses were taken daily from the clarifier as well as from each module. To gain representative samples a tube was installed into the upper part of each module from which the samples were taken (Figure 7). The NH_4-N (DIN EN ISO 6878), NO_2^--N (DIN EN ISO 11732) and NO_3-N (DIN EN ISO 13395) analyses were done by using an auto analyzer (SKALAR, Netherlands). COD and total suspended solids were measured according to DIN ISO 15705 and DIN 38409-2.

The pH value was measured daily in the clarifier by using a HQ 40d multi (Hach, Germany) with an Hach intellical phc 101 electrode (Hach, Germany). Random checks inside the modules showed, that the pH-value inside the modules was in general about 0.1 – 0.2 higher than in the clarifier. The oxygen concentration inside the bulk liquid was measured via optical oxygen measurement with light cable by using a Fibox 3 LCD-trace (PreSense, Germany), with dots at the top and bottom of each module.

To sample the air leaving the modules on the top (mixing air, stripping air and scouring air), a second tube was installed into the headspace of each module that reached into the module. Two samples

were taken before and one directly after a mixing circle, this was done three times per week. For sampling, 21 mL glass vials were hermetically sealed with butyl septum, crimped with aluminum rings and evacuated to -70kPa. Then 10 mL of sampled air was brought into the vials by using a syringe. Samples for N_2O and CO_2 were taken this way. Since no major differences between the samples that were taking before and after the mixing were detected, a mean of the three values was used for the calculations. The outlet tubes of the effluent from the modules were completely submerged in the clarifier to make sure that no air is lost through the clarifier. For sampling process air out, one tube with a needle was plugged onto the outlet of NV1 to bring the air flow into an evacuated glass tube, while a second needle was put into the butyl septum of the glass vial and left with an open end (flushing method according to Parravicini et al., 2015). Thereby an air flow through the glass vial was built up and it was made sure, that no ambient air comes into the system. With the minimum process air out flow of 1L/h, the air retention time for the 21mL tube was about 8 seconds. Since the sampling duration was 30 minutes, high representative samples were achieved.

The content of N_2O in the gas samples was measured via GC-MS (Thermo Fisher Scientific, USA), the same was done for CO_2. The oxygen content in the process air off was measured in-line by using an optical IDS dissolved oxygen sensor FDO 925 (WTW, Germany).

Mass balances for NH_4-N, NO_2^--N and NO_3-N were done for selected operation periods, Eq. 3 is for a single module while Eq. 4 is for the whole MABR system including the clarifier.

$$c_{F,i} * \dot{V}/_3 + 2 * c_c * \dot{V}/_3 - \left[c_{M,i} * \dot{V} + \left(c_{M,i+1} - c_{M,i}\right) * V_M\right] = m_{removed} \quad \text{Eq.3}$$

$$c_F * \dot{V} = c_C * \dot{V} - \left[\left(c_{C,i+1} - c_{C,i}\right) * V_C\right] = m_{removed} \quad \text{Eq.4}$$

$c_{F,i}$	concentration of the component in the feed (SDE) at process day i [g/L]
$c_{C,i}$	concentration of the component in the clarifier at process day i [g/L]
$c_{M,i}$	concentration of the component inside the module at process day i [g/L]
$\dot{V}$	volume flow rate of the feed [L/d]
V_M	volume of the module [L]
V_C	volume of the clarifier [L]
$m_{removed}$	load of removed component [g/d]

Oxygen balances were done, including OTE (Eq. 5) and OTR (Eq. 6)

$$OTR = O_{2\ process\ air\ in} - (O_{2-process\ air\ out} + O_{2\ stripping\ air}) \quad \text{Eq.5}$$

$$OTE = \frac{OTR}{O_{2\ process\ air\ in}} = \frac{O_{2\ process\ air\ in} - (O_{2\ process\ air\ out} + O_{2\ stripping\ air})}{O_{2\ process\ air\ in}} \quad \text{Eq.6}$$

OTR	[g/d]
$O_{2\ process\ air\ in}$	[g/d]
$O_{2\ process\ air\ out}$	[g/d]
$O_{2 stripping\ air}$	[g/d]
OTE	[-]

The oxygen demand for the bacteria by converting NH_4 to NO_2^+ and NO_3 was calculated with stochiometric factors for nitritation and nitrification (from Eq.7 and Eq.8) as follows:

$$O_{2-nitrification} = (c_{NO3,M} * \dot{V}) * 4.3$$ Eq.7

$$O_{2-nitritation} = (c_{NO2,M} * \dot{V}) * 3.2$$ Eq.8

$c_{NO3,M}$ concentration of NO_3 in the module [g/L]
$c_{NO2,M}$ concentration of NO_2 in the module [g/L]

Air fluxes for the oxygen balance were normalized to standard conditions (273.15°K, 101.325kPa) using Eq.9.

$$\dot{V}_{corr} = \dot{V}_{measured} * p_{in} * \frac{273,15}{273,15+T°C}$$ Eq.9

$\dot{V}$ Oxygen flux [L/d]
p_{in} Pressure before the membranes [kPa]
T Temperature [°C]

Eq.10 was used to calculate the oxygen load in the air streams in gO_2/d

$$Oxygen\ load = \dot{V}_{corr} * \varphi_{oxygen} * \frac{1}{V_{gas}} * M_{oxygen}$$ Eq.10

$Oxygen\ load$ [g/d]
φ_{oxygen} Volume fraction [-]
V_{gas} volume of a mole of gas under standard conditions = 22.4L/mol
M_{oxygen} molar mass of oxygen [g/mol]

To calculate the expected process air out flow rate of the membranes, Eq.11 was used (Parravicini et al., 2015), while x_{H2O} was taken as zero.

$$process\ air\ out = \frac{process\ air\ in*(x_{N2}+x_{Ar})_{intake\ air}}{(1-(x_{CO2}+x_{O2}+x_{H2O})_{off\ gas})}$$ Eq.11

x_{N2} mole fraction of N_2 [-]
x_{Ar} mole fraction of Ar [-]
x_{H2O} mole fraction of H_2O [-]

Henry's law (Eq. 12) was used for calculation of the concentration of N_2O inside the bulk liquid, where the Henry constant for N_2O in water is 0.025mol/L*bar (NIST, 2017).

$$p_i = K_{H,N2O} * c_i$$ Eq.12

p_i partial pressure of component i [bar]
$K_{H,N2O}$ Henry constant for N_2O [mol/L*bar]

4 Results

4.1 Plant Performance

Figure 9 shows the amount of NH_4-N inside each module as well as in the clarifier, the concentration of NH_4-N in the feed, the pH value as well as the NH_4-N loading rate of the feed.

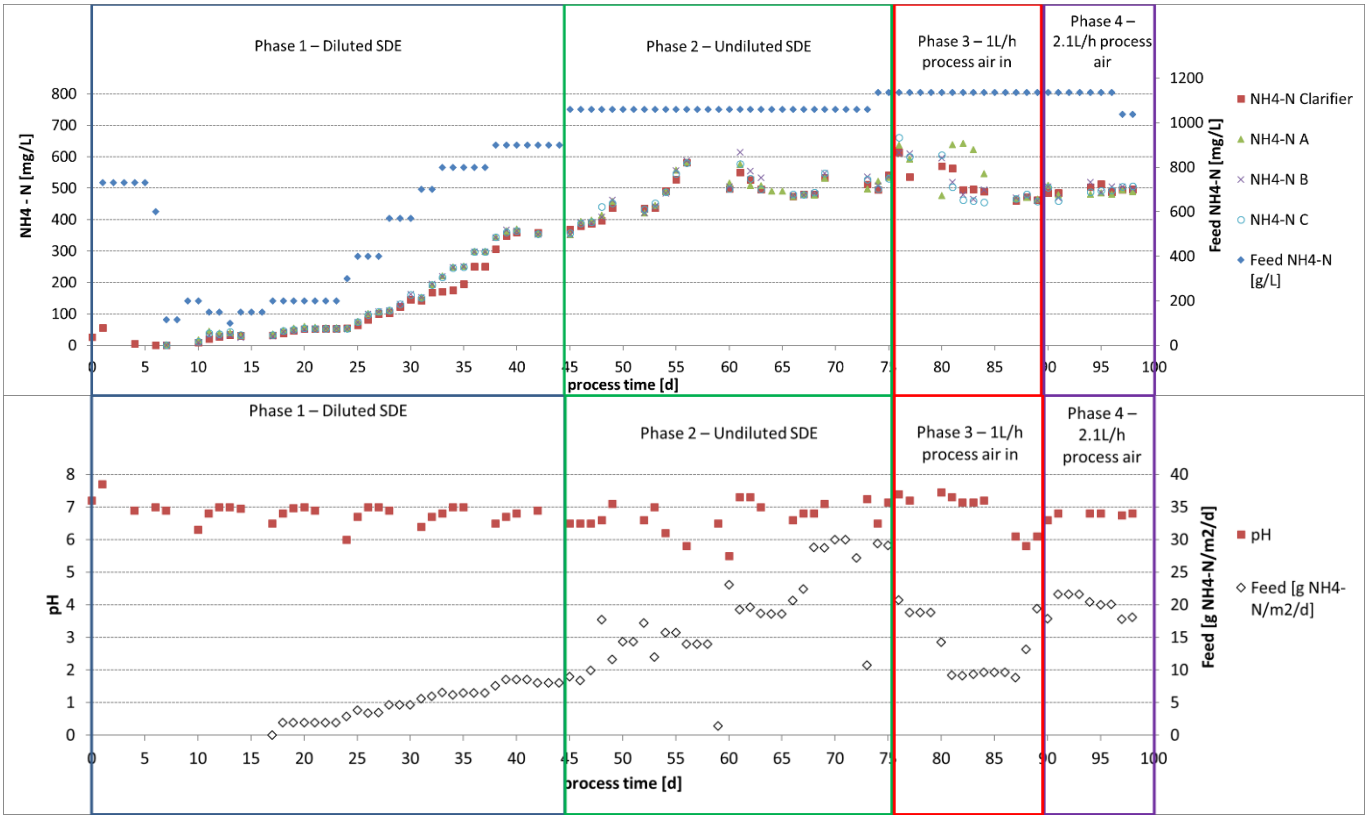

Figure 9 NH4-N concentration inside the clarifier and in each module; concentration and loading of the feed and pH value in the clarifier over full process time

Diluted SDE with increasing concentration was used for operation phase 1 (until process day 44). Acid is formed due to nitritation and alkalinity is consumed (Eq.1). So, the higher the activity of the AOBs is, the more the pH value decreases (with constant loading rate in the feed). Especially in operation phase 1 it can be seen, that the pH value increases after the NH_4-N loading rate was increased. After about 4 days, the pH value decreased again, due to high AOB activity. Whenever the pH value was around 6.3, the NH_4-N loading rate in the feed was increased again. Good biofilm growth was achieved with this strategy. It took 44 days to build up a biofilm that could handle undiluted feed, for that time the NH_4-N loading rate was increased linear (R^2=0.95) by 0.29g/m²/d. After 61 days, the DO was zero in all three modules for the first time, which means that the bulk liquid is an anoxic zone and it can be assumed that most of the NH_4-N conversion takes place in or near the biofilm. For the whole process time, it was made sure that the pH does not reach values above 7.3

The NH_4-N concentration inside the modules as well as in the clarifier showed quite similar behavior and increased to 380mg/L in operation phase 1.

Since process day 45 undiluted SDE was used for the rest of the process time while varying the flow rate of the feed. It was again made sure that the pH is below 7.3.

Again, the NH_4-N concentration inside the modules as well as inside the clarifier showed similar behavior and increased to an almost constant value of 515±50mg/L.

An air leakage at NV1 was detected at process day 75, revealing that much more process air had been conveyed into the membranes then the one expected based on the measurements in process air out. After the fixing of the leakage and the followed decrease of the process air to 1L/h, a limitation due to oxygen led to a decrease of the activity of the bacteria and therefore an increase of the pH value.
This was the start of operation phase 3. To prevent FA inhibition, the NH_4-N loading rate was decreased to 1.9g NH_4-N/m²/d until the pH value dropped to 6 (process day 87). The NH_4-N loading rate was then increased again.
The process air was increased to 2.1L/h at process day 89, which started operation phase 4. The NH_4-N loading rate in the feed was increased to 22 NH_4-N/m²/d which lead to a constant pH of 6.8.

The oxygen concentration inside the bulk liquid (Figure 10) was almost constant at 8.7±0.77mg/L for the top and 8.5±0.8mg/L for the bottom of the modules for process time 1-28 and decreased until it reached 0 for all three modules at process day 61 for the first time. The gap of 0,2mg/L between top and bottom can be explained with higher oxygen concentration of the process air at the top of the module. Therefore, the oxygen concentration in the bulk liquid at the top is higher than at the bottom.
The blocking of the feed due to clogging at process day 54, 56 and 60 as well as the blocking of module A at process time 80 lead to an increase of the DO in the bulk liquid.
At the beginning of operation phase 4 (process day 89) process air in was increased from 1L/h to 2.1L/h, the NH_4-N loading rate in the feed was reduced from 19gNH_4-N/m²/d at process day 89 to 18gNH_4-N/m²/d at process day 90, still the DO did not reach values above 0 which indicates an oxygen limitation in operation phase 3.

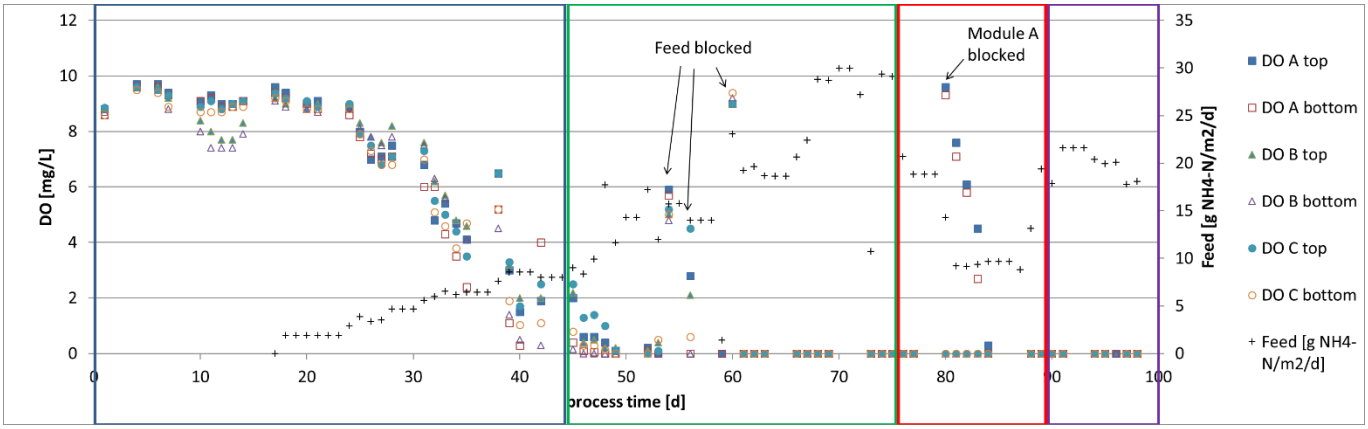

Figure 10 DO of all three modules and NH_4-N loading rate over full process

Figure 11 shows the amount of nitrite (NO_2^--N), nitrate (NO_3-N) and the amount of ammonium (NH_4-N) inside module A over the entire process.

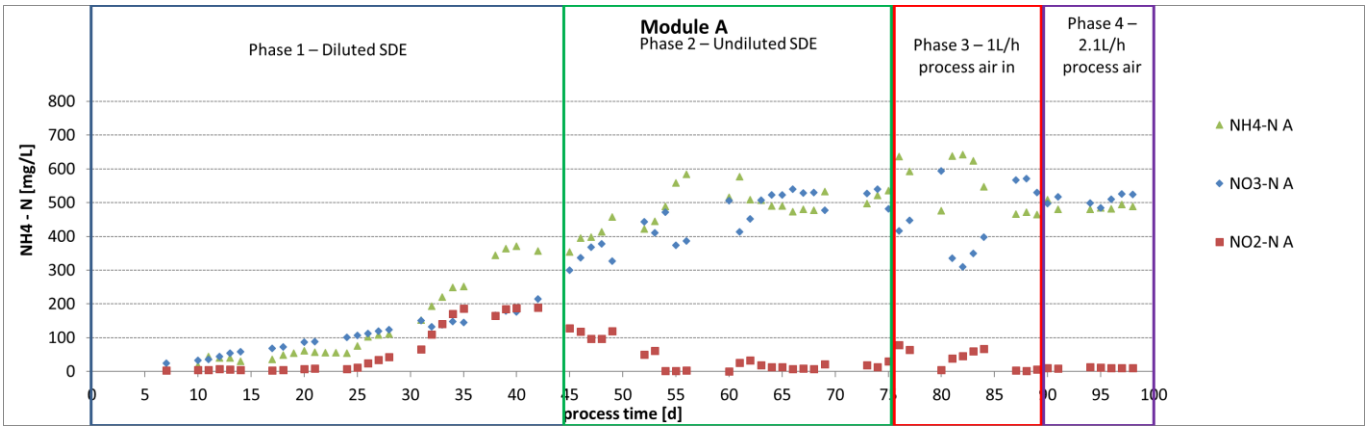

Figure 11 NH_4-N, NO_3-N, NO_2^--N in module A over entire process time

NO_2^--N is increasing from process time 25 to 35, and then again decreasing to 0 at process time 54. Small amounts of NO_2^--N can be detected at process time 75 and 80, but decreased to zero again at process time 87.

NO_3-N is steadily increasing, from operation phase 2 until the end of the process, NO_3-N and NH_4-N values are about the same, which speaks for complete nitrification with a conversion rate of 50%. The only exception is at process time 80 - 84, where 13 - 78mg NO_2^--N /L were detected, the NO_3-N concentration decreased to 335 – 397mg NO_3-N/L at this time. After the loss of NO_2^--N, also NO_3-N increased again, to values around the NH_4-N concentration.

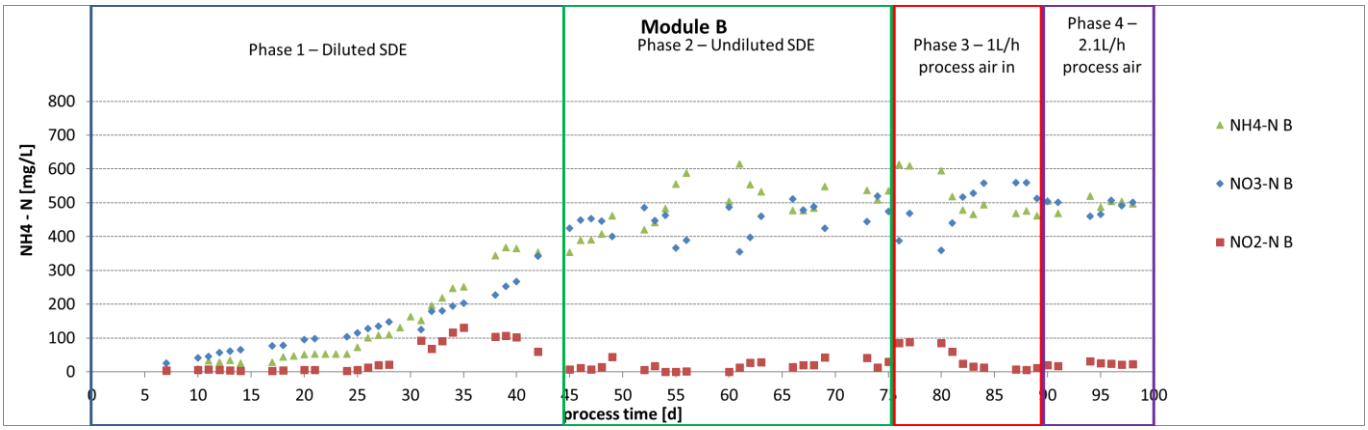

Figure 12 NH_4-N, NO_3-N, NO_2^--N in module B over entire process time

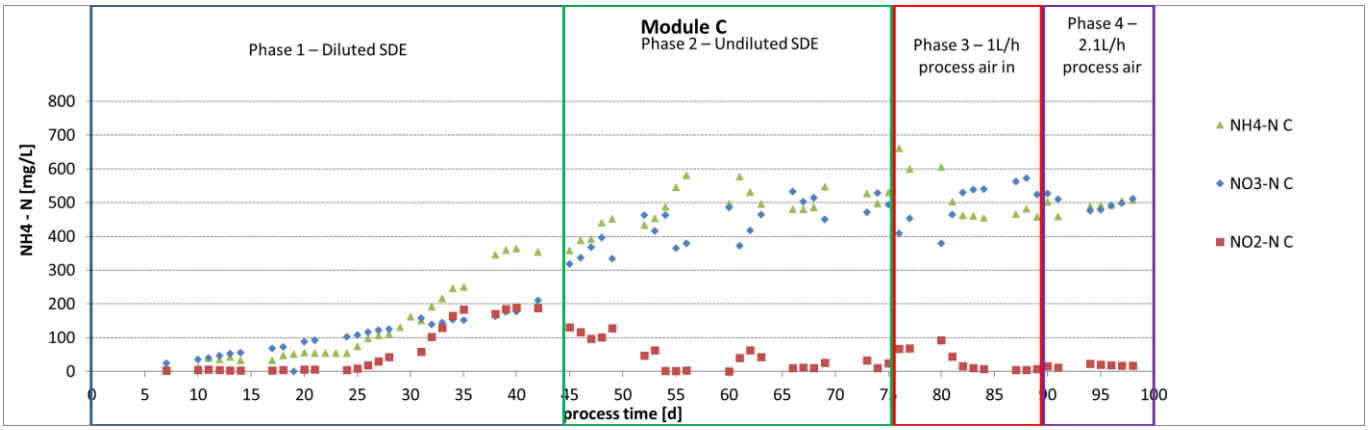

Figure 13 NH_4-N, NO_3-N, NO_2^--N in module C over entire process time

Figure 12 and Figure 13 show the same measured parameters as Figure 11 but for Module B and C. While the behavior between the three modules was quite similar, two major differences can be seen. First, the NO_2^--N concentration in module B at the end of operation phase 1 is decreasing faster than in module A and C and reaches zero at process time 45 (module A and C at process time 54 or 52). The different behavior of module B in this period could might be explained with the chord setup. The chords in module A and C were straight and loose inside the reactor, while the chords inside module B were twisted and more tight, which could lead to a decrease of the cord surface that is in touch with the bulk liquid. Investigations were done during the process to make sure that the feed gets pumped into each module equally.
Second, the NO_2^--N concentration in module A at process day 80 reaches zero before it rises again, while the NO_2^--N concentration in module B and C do not drop to zero at process day 80. Also, the NH_4-N concentration in module A is decreasing at process day 80 due to the blocking of the module. While the NH_4-N concentration in module B and C is decreasing at the following process days (450 – 500mg NH_4-N/L), the concentration inside module A rises to 620mg/L.

4.2 Free ammonia (FA) and free nitrous acid (FNA)

Figure 14 shows the amount of free ammonia (NH_3-N) on the primary axis and the amount of ammonium in the modules on the secondary axis. The box indicates the threshold for start of inhibition of the NOBs at 0.1 – 1mg NH_3-N /L (Anthonisen, et al., 1972). Anyway, these values are neither representative for MABR technology nor for SDE treatment, so comparability is limited.

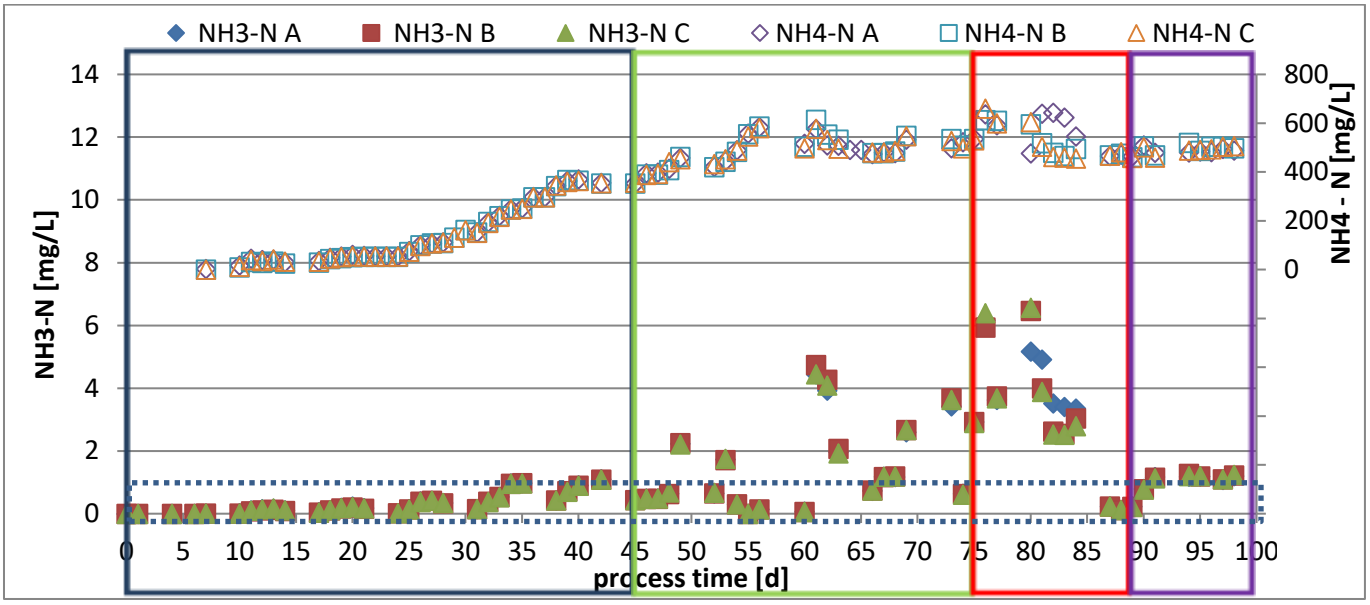

Figure 14 FA (NH_3-N) concentration of each module over the full process time on primary axis; NH_4-N concentration of each module over the full process time on secondary axis; the box indicates the threshold for inhibition of NOBs

Figure 15 shows the same as Figure 14 but NO_2^--N instead of NH_4-N is shown on the secondary axis. The first peak of the NH_3-N for all three modules can be seen at process day 62, which happened due to a pH value of 7.3. The increase of the pH happened due to the blocking of the feed at process day 59. Since module A was blocked, no feed was pumped into module A but all into module B and C. Therefore, the NH_4-N loading rate for module B and C was increased drastically, which lead to an increase of the pH value in the clarifier.
After the increase of the NH_4-N loading rate at process day 60 and 61, the pH value increased to 7.3. Another peak of the NH_3-N concentration can be seen at process day 76. This can again be explained

with an increase of the pH value. After it was fixed, the process air was decreased to 1L/h, which lead to an increase of the pH value due to oxygen limitation of the biofilm.
A third peak occurred at process day 80, where module A was blocked and therefore the pH value increased. After fixing of the blocking, the NH_3-N concentration decreased again.
Anthonisen reported, that AOB inhibition starts at FA 10-150mgNH_3-N/NL, which is far from the values in this study.

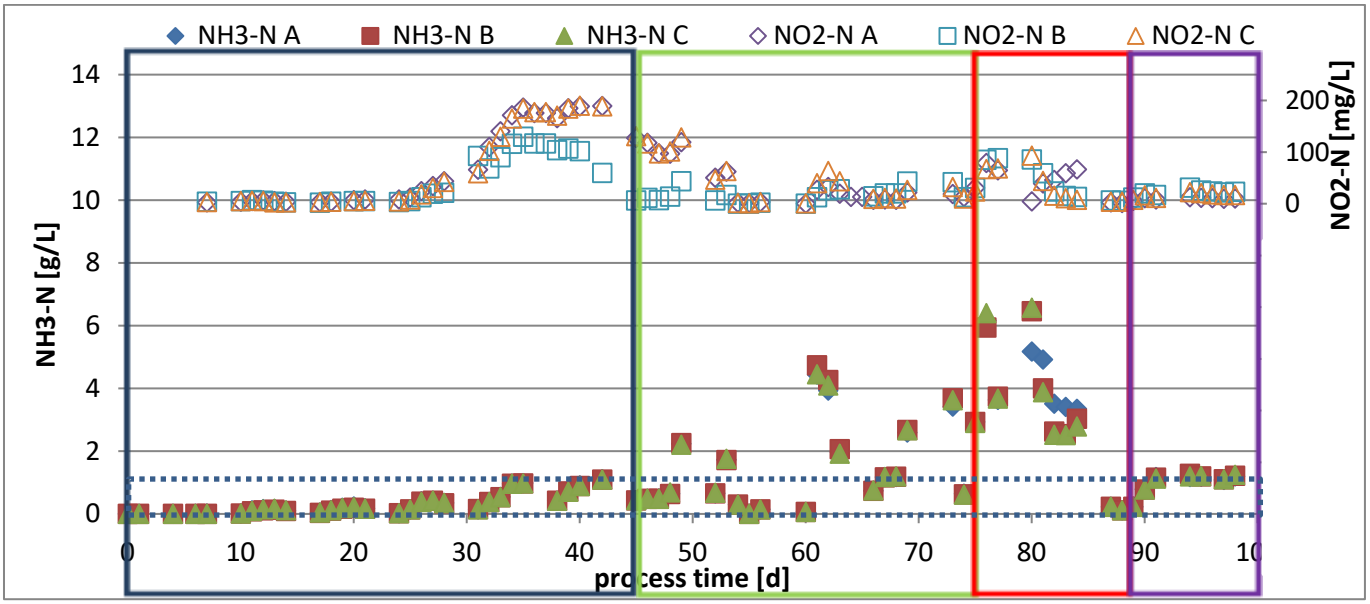

Figure 15 FA (NH_3-N) concentration of each module over the full process time on primary axis; NO_2^--N concentration of each module over the full process time on secondary axis; the box indicates the threshold for inhibition of NOBs

Figure 16 shows the amount of free nitrous acid FNA (HNO_2) on the primary axis and the amount of nitrite in the modules on the secondary axis. The box indicates the threshold for complete inhibition of the NOBs at 0.026 - 0.22mgHNO_2/L (Zhou, 2011), while those tests were neither performed with biofilm nor SDE. It can be seen, that the HNO_2-N concentration in the modules is over the threshold for inhibition of NOBs, while still no inhibition was achieved.
A 50% reduction of AOB activity was observed in a range of 0.42 – 1.72mgHNO_2-N/L (Zhou, 2011), which is again, except for process day 38, far from the values for the process.

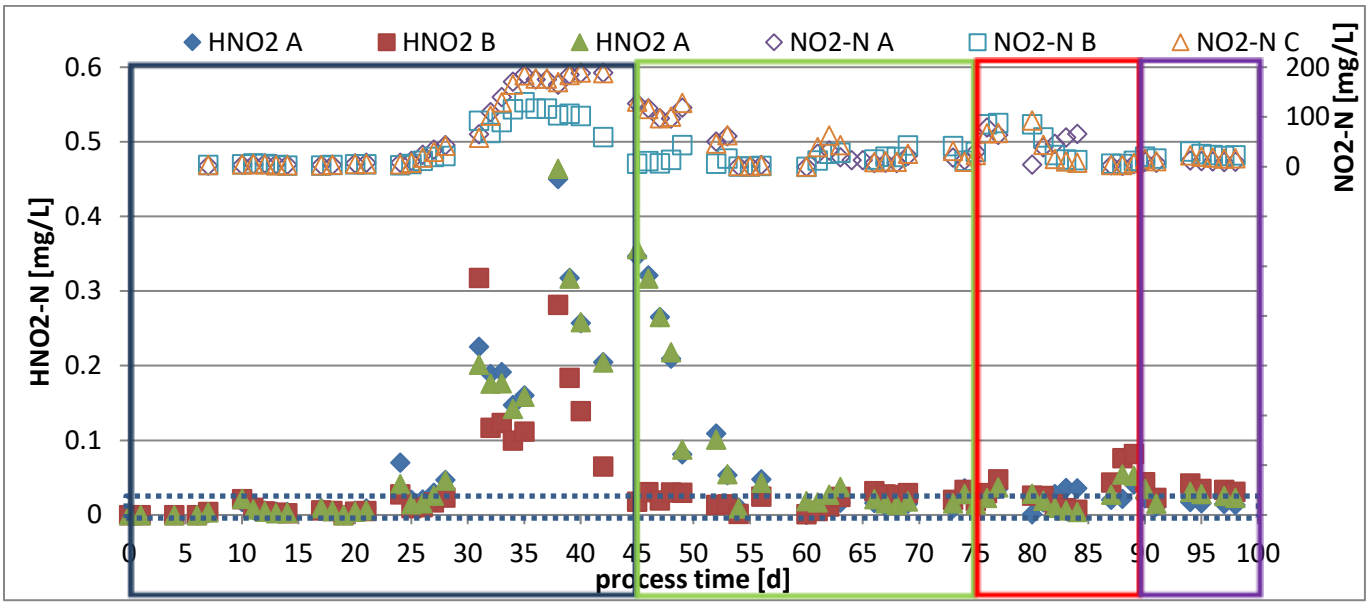

Figure 16 FNA (HNO_2-N_l) concentration of each module over the full process time on primary axis; NO_2^--N concentration of each module over the full process time on secondary axis; the box indicates the threshold for inhibition of NOBs

4.3 Ammonium removal rate and performance metrics

Figure 17 shows the NH_4-N removal rate over the entire process time for each module.

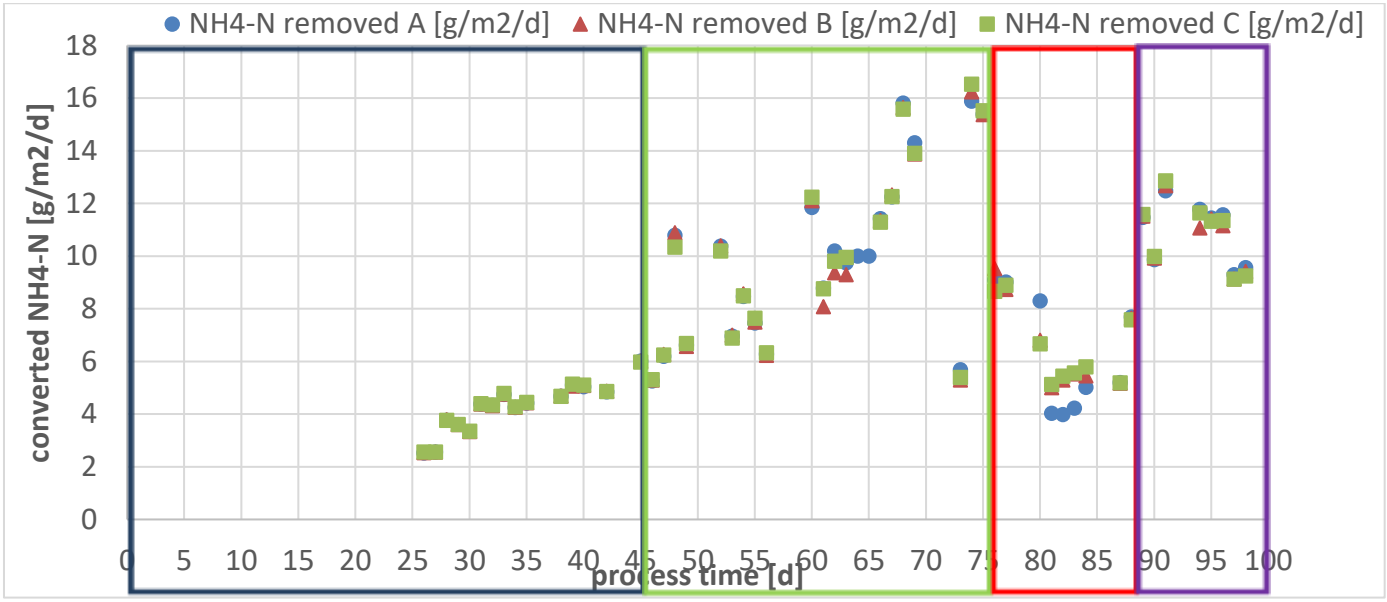

Figure 17 NH_4-N removal in each module over the entire process time

Eq.4 was used for the calculation of the values shown in Figure 17. The peaks at process time 48, 52, 60, 66, 68 and 91 can be explained with the increase of the NH_4-N loading of the feed and the hydraulic retention time of the plant. At these process days, the NH_4-N loading was increased while the concentration inside the modules did not increase immediately due to the hydraulic retention time. The high NH_4-N removal rate at these days can therefore be seen as some kind of outliers. The minimum values at process time 56 and 73 can be explained with the blocking of the feed. At process time 80, module A was blocked, therefore the NH_4-N concentration decreased in module

A, while it increased for module B and C. Through that, the high values for module A and the low values for module B and C can be explained.
Apart from the values explained above, the NH_4-N removal rate increased quite constantly until process day 74 where it had its maximum (16.5gN/m²/d removed). The NH_4-N removal rate decreased at operation phase 3, since the NH_4-N loading rate in the feed and the process air in were decreased. Still, a fast increase of the removal rate at the end of operation phase 3 and at the beginning of operation 4 can be seen. At the end of process phase 4 9.2g/NH_4-N/m²/d were removed. The decrease of the removal rate at process 97 and 98 can be explained with the decrease of the NH_4-N loading in the feed (Figure 10).

Performance metrics of NH_4-N removal rate, the ratio of the converted NH_4-N and the NH_4-N loading in the feed and the ratio of NO_2^--N with the converted NH_4-N for the system are shown in the following tables (Table 2, Table 3, Table 4 and Table 5). Process time 33-37 (operation phase 1), 61-65 (operation phase 2), 80 – 84 (operation phase 3) and 94 – 98 (operation phase 4) were chosen for calculating the metrics due to constant feed at this process time. These metrics were chosen since they describe two of the three targets of the thesis (ammonium removal, partial nitrification) the best.

Table 2 Performance metrics for process days 33 - 37

	NH_4-N removal rate [g/m²/d]	NH_4-N_{conv} /NH_4-N_{feed}	NO_2^--N/ NH_4-N_{conv}
Module A	3.8 ± 0.7	0.75 ±0.03	0.21 ±0.03
Module B	3.9 ± 0.7	0.75 ±0.03	0.14 ±0.02
Module C	3.9 ± 0.8	0.75 ±0.03	0.21 ±0.03
Total	3.8 ± 0.6	0.75 ±0.03	0.19 ±0.04

The performance metrics for process day 33 – 37 (operation phase 1) are shown in Table 2. The NH_4-N loading rate of the feed was at 6.5 gNH_4-N/m²/d. A total NH_4-N removal rate of 3.8gNH_4-N/m²/d can be seen for this process time. This means, that 75% of the NH_4-N in the feed was converted, while 19% were converted to NO_2^-.
Eq.4 was used to calculate the load of NO_2^+, NO_3 and NH_4 in the outlet. With those, an N balance was calculated and its gap expressed as:

$$balance\ gap = \frac{NH_4in-(NO_3out+NO_2out+NH_4out)}{NH_4in} \quad \text{Eq.13}$$

The N- balance showed a gap of 55% for process time 33- 37. This high value can be explained with the increase of the NH_4-N loading rate in the feed in the time before the balance. Due to high hydraulic retention time in operation phase 1, it takes time until the feed goes through the modules into the clarifier, which could be reason for the gap. Investigations regarding COD removal showed, that 50mg/L were removed. 2.9 mg COD are needed to remove 1mg of NH_3 (Yoon, 2015), which means that 17.2mgNH_3-N/L could have been removed. This means that the impact of denitrification on the N balance is vanishingly low and can therefore not be the reason for the gap.

Table 3 Performance metrics for process days 61 - 65

	NH_4-N removal rate [g/m²/d]	NH_4-N_{conv} /NH_4-N_{feed}	NO_2^--N/ NH_4-N_{conv}
Module A	7.6 ± 1.3	0.52 ±0.03	0.03 ±0.02
Module B	7.1 ± 1.2	0.51 ±0.04	0.04 ±0.02
Module C	7.3 ±1.2	0.52 ±0.03	0.05 ±0.03
Total	7.3 ±1.3	0.52 ±0.03	0.04 ±0.03

The performance metrics for process days 61 – 68 (operation phase 2) is shown in Table 3. The NH_4-N loading rate at this time of the process was at 19.2 – 22.4gNH_4-N/m²/d. A total NH_4-N removal rate of 7.3g/m²/d can be seen for the balance. Due to a blocking of the feed at process day 59 and changing of the feed at process day 60 and 61 the values given in Table 3 vary from the results shown in Figure 17. While about half of the NH_4-N (0.52) was converted into NO_3-N, almost no NO_2^--N (0.04) accumulated.

The N-balance for process day 61 – 65 had a gap of 6%.

Table 4 Performance metrics for process days 80 - 84

	NH_4-N removal rate [g/m²/d]	NH_4-N_{conv} /NH_4-N_{feed}	NO_2^--N/ NH_4-N_{conv}
Module A	1.7 ±1.0	0.43 ±0.04	0.1 ±0.05
Module B	4.7 ±0.5	0.55 ±0.01	0.03 ±0.01
Module C	5.5 ±0.2	0.57 ±0.003	0.02 ±0.01

The performance metrics shown in table Table 4 are at process time 82 – 84 (operation phase 3), where the NH_4-N loading rate was at 9.5g NH_4-N/m²/d. The low NH_4-N removal rate in Module A can be explained with the blocking of the module at process day 80.
The conversion rate of the removed NH_4-N to NO_2^--N is at low values (0.02 – 0.1), so total nitrification took place at this time of the process, while almost no NO_2^--N accumulated inside the modules.
As mentioned above, a N-balance was done for process time 82 – 84, and showed a gap of 1%.
Due to the big differences between Module A and B and C, no total metrics are shown for this process time.

Table 5 Performance metrics and NH_4-N removal rate for process days 94 - 98

	NH_4-N removal rate [g/d/m²]	NH_4-N_{conv} /NH_4-N_{feed}	NO_2^--N/ NH_4-N_{conv}
Module A	11.7 ± 1.6	0.54 ±0.01	0.02 ±0.002
Module B	10.2 ±2.0	0.52 ±0.01	0.05 ±0.01
Module C	11.3 ±1.4	0.53 ±0.01	0.03 ±0.004
Total	11.1 ±1.5	0.53 ±0.01	0.03 ±0.01

For process time 94 – 98 the plant showed the maximum performance for a set process air flow rate. With a feed rate of 20.3gNH_4-N/m²/d the plant showed an ammonium removal rate of 11.7 g/d/m² for module A, 10.2 g/d/m² for module B and 11.3 g/d/m² for module C. This means, that 11.1gNH_4-N/d was removed in total.
The conversion rate of the removed NH_4-N to NO_3-N is similar to the ones shown in Table 4. This means that total nitrification took place.
The gap for the N-balance was 10%.

4.4 Oxygen balance, OTE and OTR

Reliable air measurements were obtained for operation phase 3 and 4 and oxygen balances were done for these process days. For the process air in ROT1 was used, a gas meter (in operation phase 3) and the method of the water displacement column (operation phase 4) was used for process air out. Table 6 shows the characteristics of the air flows. It can be seen, that input and output flow rates vary significantly. Since process air in is expected to be the same as process air out (about the same amount of consumed oxygen was detected as CO_2 via GC-MS), two balances were done, once with the input values and once with the output values. Eq.11 was used to validate the assumption, that the flow rate of process air in = process air out. Therefore it was assumed, that denitrification is negligible and that the system is in steady state. The law of mass conversion says, that $n_{N2} + n_{Ar}$ of the process air in needs to be the same as $n_{N2} + n_{Ar}$ in process air out (Parravicini et al., 2015). The results of the calculation are shown in Table 6.

The characteristic of the air flows is shown in Table 6, the oxygen concentrations of the process air out is shown in Table 7. For the calculations using the air flow rate of the air flow out, stripping air needs to be considered which is already done Table 6. No values regarding stripping air are available for operation phase 3, therefore an airflow rate of 2NL/d is assumed.

Table 6 characteristics of the air flow for process phase 3 and 4 and calculated air flow rates

	Air flow rate [NL/d]	Air flow rate calculated [NL/d]
Process air in (process phase 3)	29.8	30.0 ±1.4
Process air in (process phase 4)	60.1	60.8 ±0.2
Process air out (process phase 3)	13.0	13.1 ±0.5
Process air out (process phase 4)	49.6	50.2 ±0.2

Table 7 Oxygen concentration of process air out for operation phase 3 and 4

Process day	oxygen concentration [%]	Operation phase
76	6.5	3
77	8.4	3
80	12.3	3
81	12.6	3
82	14.5	3
83	15.9	3
91	17.1	4
94	17.4	4

The increase of the oxygen concentration inside the process air out from process day 77 to 80 can be explained with the decrease of the NH_4-N loading of the feed (Figure 10). In process phase 4, the NH_4-N loading rate of the feed was increased again, but also the process air flow was increased from 1L/h to 2.1L/h. Therefore, the oxygen concentration in process air out increased again.

Eq.7 and Eq.8 were used to calculate the oxygen demand of the bacteria. The oxygen concentration in the process air out was measured and used for the balance, further the oxygen concentration in the stripping air was measured at a later process time and showed no significant differences between stripping air and process air out. Therefore, the same oxygen concentration as for process air out will be used for stripping air in the calculation.

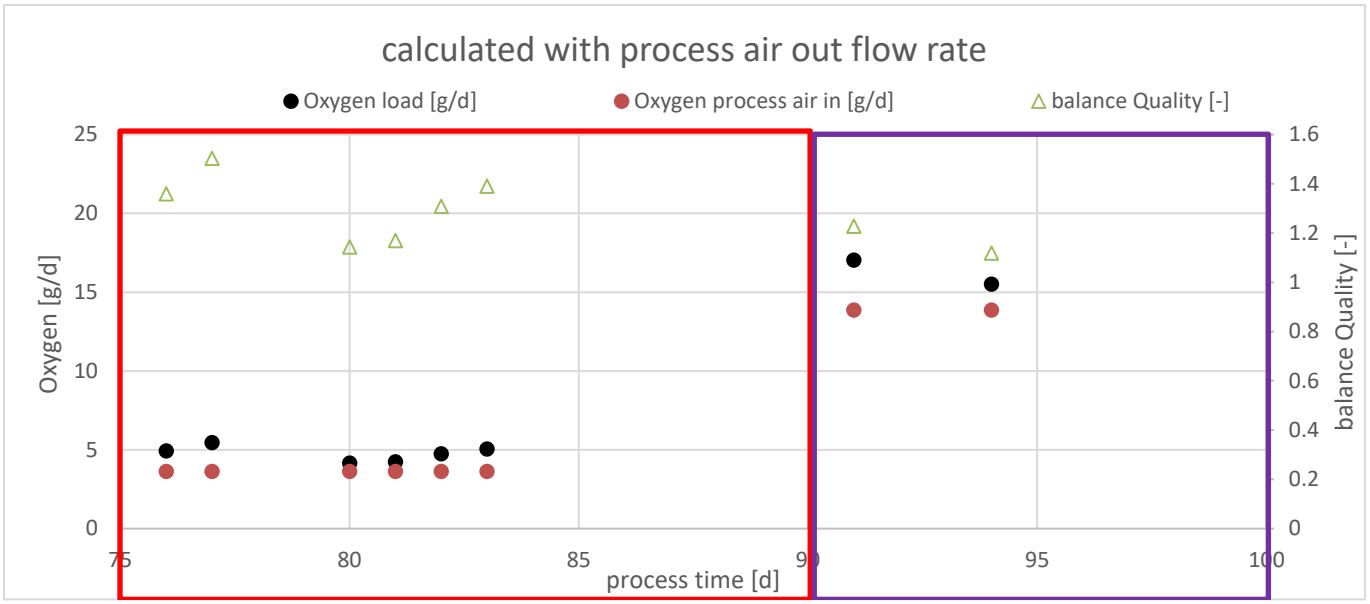

Figure 18 Oxygen balance for operation phase 3 and 4 calculated with the output flow

Figure 18 shows the oxygen balance for operation phase 3 and 4. Oxygen load is the amount of oxygen in process air out and the demand of oxygen from the bacteria for nitrification. The balance was calculated with the air flow rates of process air out. Eq.7 and Eq.8 were used to calculate the oxygen demand of bacteria. The balance shows a quality of 1.3±0.1 for operation phase 3 and 1.17±0.08 for operation phase 4.

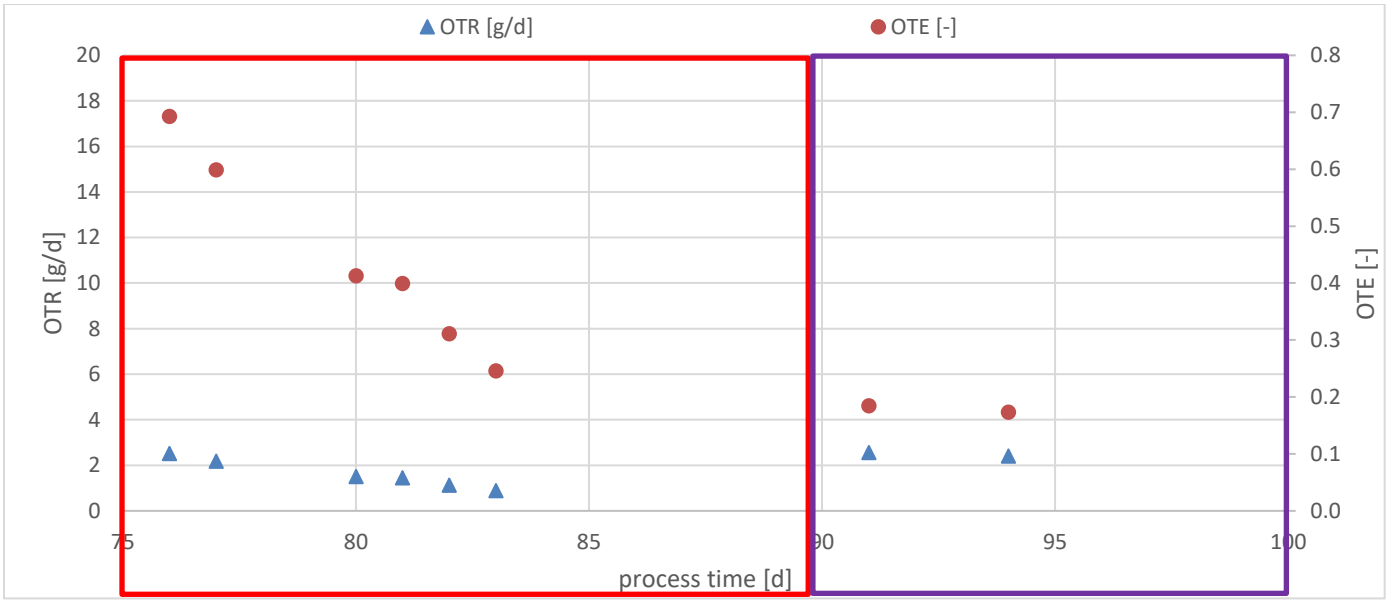

Figure 19 OTE (secondary axis) and OTR (primary axis) for operation phase 3 and 4, calculated with the process air out flows

Figure 19 shows OTE and OTR for operation phase 3 and 4, calculated with the air flow rates of process air out. OTE and OTR was calculated for each day, where the oxygen concentration in the out flow was measured.

In operation phase 3, OTR started with 2.52 gO_2/d and constantly decreased to 0.89 gO_2/d. OTR shows the maximum at process day 91 with 2.55 gO_2/d.

OTE started with 0.7 at process day 76 and decreased constantly to 0.25 at process day 83. In operation phase 4, the OTE arrived at the minimum of 0.17.

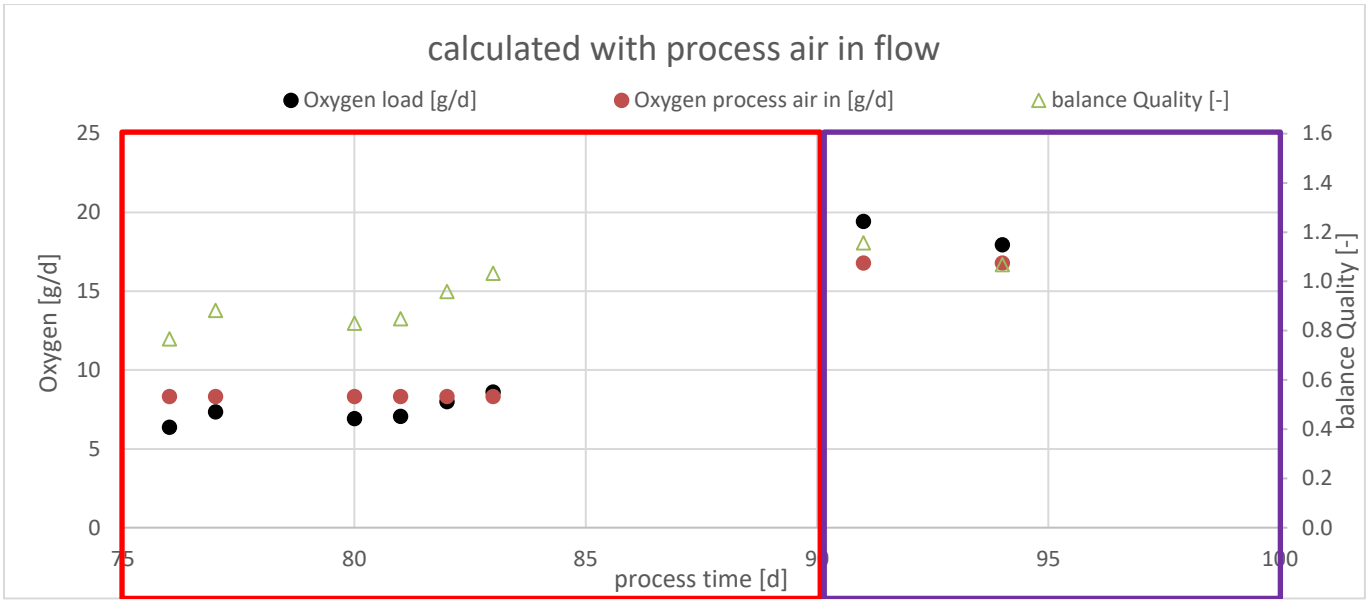

Figure 20 Oxygen balance for operation phase 3 and 4 calculated with the input flow

Figure 20 shows the oxygen balance for operation phase 3 and 4. With a balance quality of 0.9±0.1 the result is better than as the one calculated with the output flow rates.

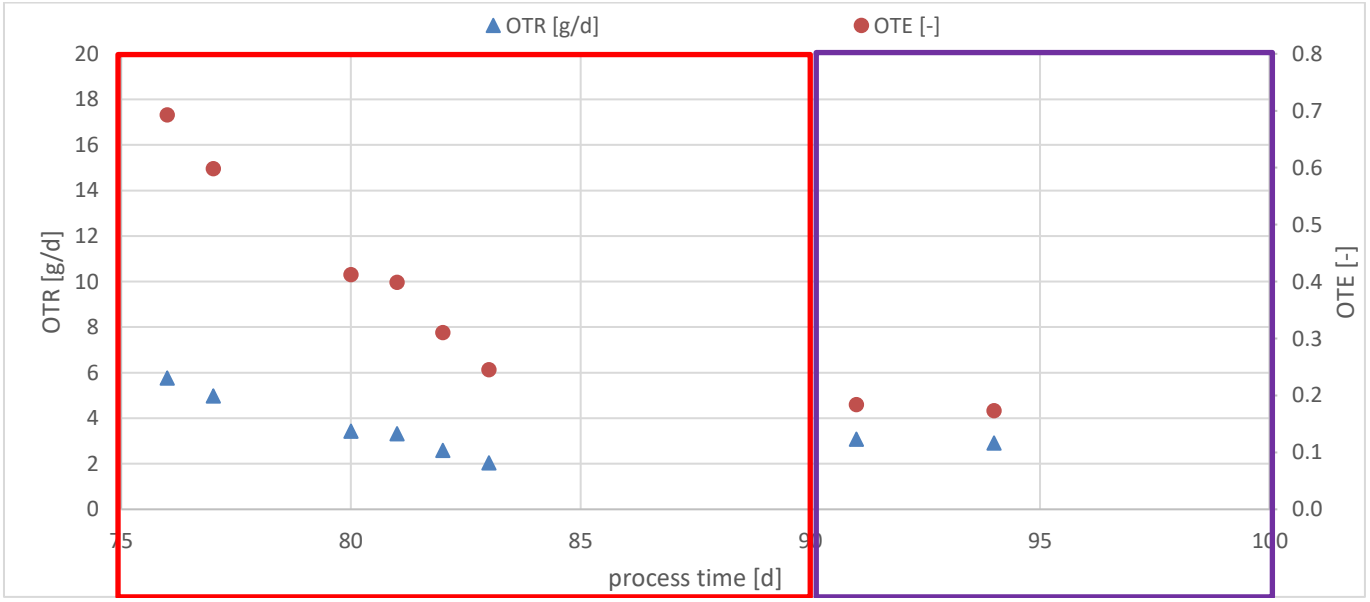

Figure 21 OTE (secondary axis) and OTR (primary axis) for operation phase 3 and 4, calculated with the process air in flows

Figure 21 shows OTE and OTR for operation phase 3 and 4, calculated with the air flow rates of process air in.

OTR has the peak right at beginning of operation phase 3 with 5.8gO_2/d and decreases to 2.0 at process day 83. In operation phase 4, OTR increases again and has values around 3.0g O_2/d. The high values compared to the ones in Figure 19 can be explained with the high air flow rates for the process air in, compared to process air out (especially in operation phase 3).

OTE starts at 0.69 at the beginning of process phase 3 and decreases to 0.25 at the end of operation phase 3. The minimum is at process day 94 with 0.17.

4.5 N_2O - Emission

Figure 22 shows the N_2O content in the headspace of each module on the primary axis, the N-loading of the feed is shown on the secondary axis.

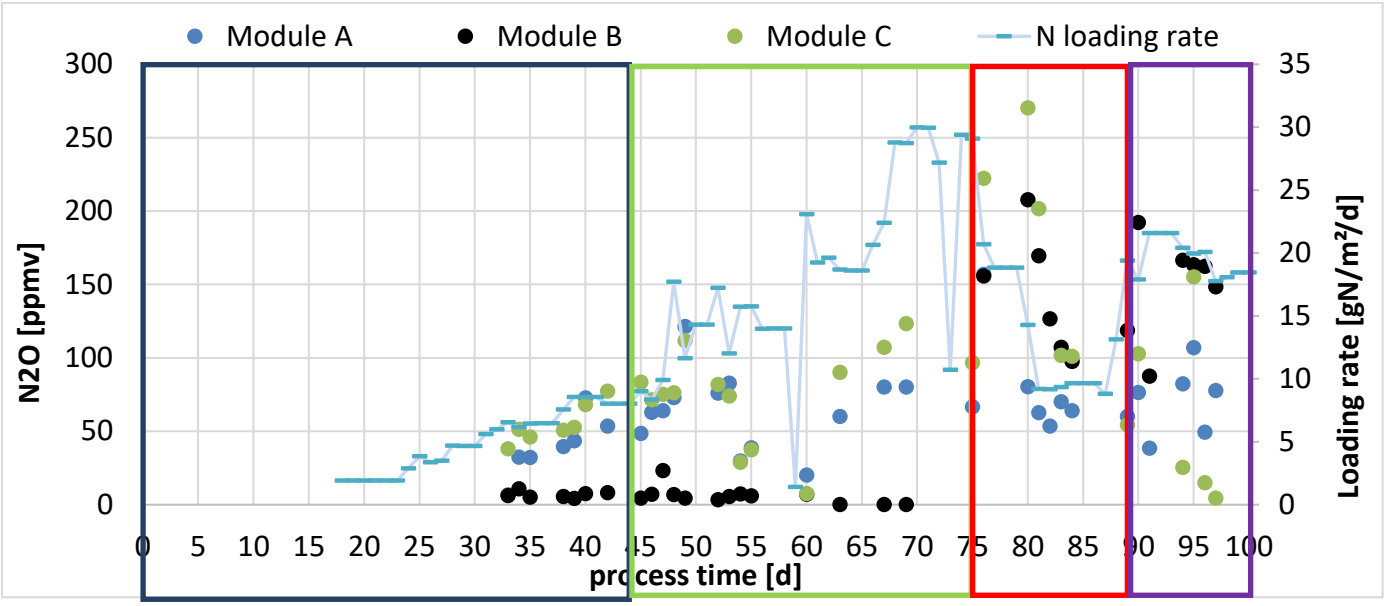

Figure 22 N2O content in the headspace of each module over the full process time on primary axis, N loading rate of the feed on the secondary axis

The N_2O emission for module A increased slightly in operation phase 1 and had a peak in operation phase 2 at process time 49 (121ppm), which is the highest value for module A for the full process time. After a decrease to 20ppm at process day 60, the N_2O emissions of module A increased to values of 60-80ppm and was almost constant in this range for the rest of the process time (operation phase 3 and 4).

Module B showed almost no N2O emissions in operation phase 1 and 2. The pressure before the membrane was significantly higher in operation phase 2 compared to operation phase 3 and 4, which might had an impact on the N_2O values measured in the headspace of module B. Also, the CO_2 values measured in the headspace of module B varied from the values measured in A and C. While the NH_4-N removal rate in module B was very similar to module A and C, the CO_2 content in module B was significantly lower than in module A and C. Anyway, the reason for the behavior of module B regarding N_2O emissions can not be given at this point.

At the start of operation phase 3 (process day 76) module B showed a value of 156 ppm N_2O and increased to 208 ppm which is the maximum for this module. For the rest of operation phase 3, the values decreased to around 90ppm. Except for process day 90 (103ppm), module B showed values between 190 and 200ppm for operation phase 4 which is the highest emission for all three modules in process phase 4.

Module A and C showed quite similar behavior for operation phase 1 and the beginning of operation phase 2. From process day 62 until the end of operation phase 2 (process day 75) module C showed in general the highest values (54 – 123 ppm). The peak of the N_2O emission for module C (and all three modules) is in operation phase 3 at process time 80 with 270ppm. After that, the values decreased again to around 100ppm at operation phase 3. In operation phase 4, module C shows one

peak (155 ppm) at process time 95, for the rest of the time, the values are close to zero Except for one value at process day 95, module C shows the lowest values of N_2O for operation phase 4.

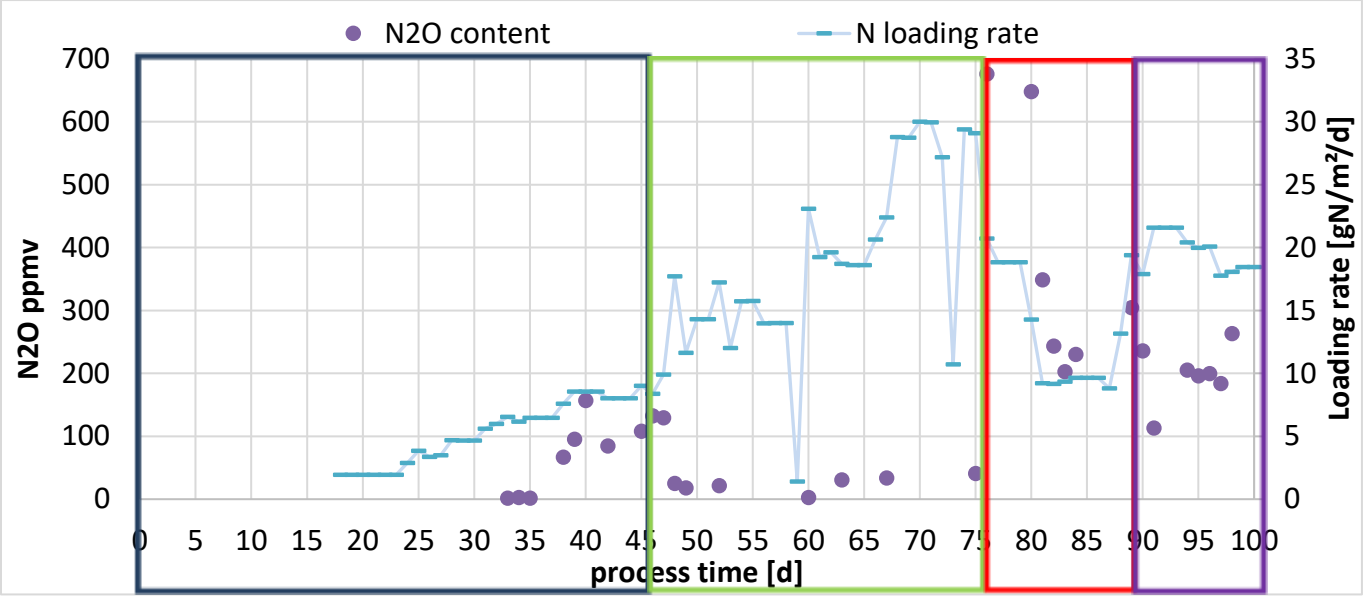

Figure 23 N2O content of the process air over the full process time on primary axis, N loading rate of the feed on the secondary axis

Process air out shows the highest values of N_2O emissions for operation phase 1, with a peak at process time 40 (157ppm). At the beginning of operation phase 2, process air out showed again higher values than the modules, but decreased rapidly at process day 49 and showed values around 50ppm for the rest of operation phase 2. It is not plausible that the N_2O values for the process air vary so significantly from the N_2O values in the module. An explanation could be, that the leakage occurred in operation phase 2. The samples for the N_2O content in the process air were taken with the flushing method after the point where the leakage occurred. Due to the higher pressure drop caused by the needles in the sampling glass vial, probably more air left the system through the leaking point and did not filled the sampling vial. This might be an explanation for the low N_2O values in operation phase 2.
In operation phase 3, process air out showed a significant increase and the maximum of the full process time at process day 76 with 676ppm. With values around 200-230ppm the emission of process air out decreased again, but is still significantly higher than the emission of the modules.

The dissolved N_2O inside each module was calculated using Henry's law (Figure 24).For this purpose, the N_2O content in the headspace was used for calculation.

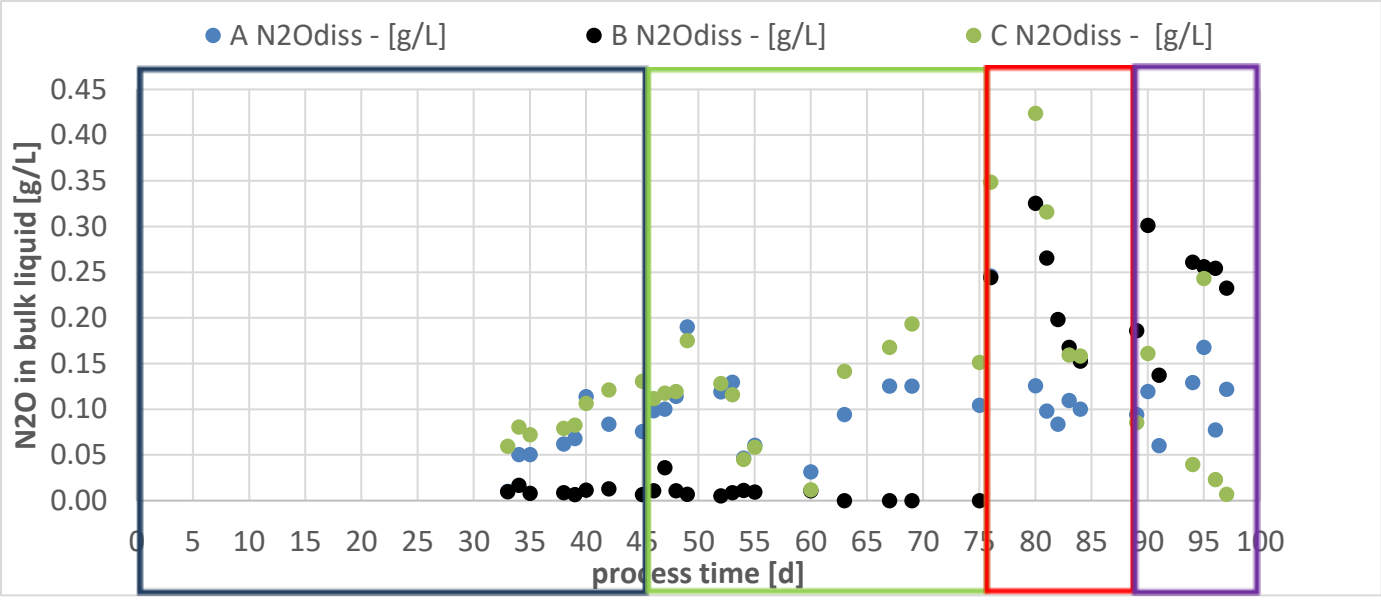

Figure 24 Dissolved N_2O inside each module, calculated with Henry's law and N_2O content in the the headspace of the modules

Since the concentration of N_2O in the bulk liquid of the modules is directly proportional to the N_2O concentration in the headspace of each module, the trend in Figure 24 is the same as in Figure 22. For operation phase 1, values between 0.05 and 0.08gN_2O/L can be seen for module A, 0.009 – 0.013gN_2O/L for module B and 0.06 – 0.12gN_2O/L for module C. For operation phase 2, values between 0.076 – 0.13gN_2O/L for module A, 0.007 – 0.036gN_2O/L for module B and 0.13 – 0.19gN_2O/L for module C can be seen. For operation phase 3, values between 0.08 – 0.25gN_2O/L for module A, 0.15 – 0.33 gN_2O/L for module B and 0.16 – 0.42 for module C, which is the maximum over the full process time. For operation phase 4, module A showed values between 0.09 – 0.16gN_2O/L, module B 0.14 – 0.26gN_2O/L and module C 0.006 – 0.24gN_2O/L.

The N_2O emissions were calculated for the same process times as the balances were done (process time 33 – 37 (operation phase 1), process time 61 – 66 (operation phase 2), process time 80 – 84 (operation phase 3) and 94 – 98 (operation phase 4)) and are shown in Table 8 - Table 11. In operation phase 1 and 2, no reliable data concerning the process air flow are available and are therefore not shown.
The mixing air, as well as the scouring air were used for calculation of the emission over the modules while process air out was used for the emission of the process air. The values were normalized on the removed ammonium as well as on the surface of the membranes.
For the calculation, an air flow of 26.4L/d/module for mixing and stripping air were used. Scouring was performed two times per day with a flor rate of 1.35L/scouring for module A, 1.73L/scouring for module B and 1.58L/scouring for module C. For calculation of N_2O-N/NH_4-$N_{removed}$ for process air, the sum of the NH_4-N removal rate of all three modules were used.

Table 8 N_2O emission over modules and process air off for process day 33 - 37

	N_2O-N [g/d/m²]	N_2O-N/ NH_4-N_{conv} [%]
Module A	0.025 ±0.010	0.7 ±0.3
Module B	0.007 ±0.002	0.2 ±0.09
Module C	0.05 ±0.003	1.3 ±0.31

Table 8 shows the N_2O emission for process time 33 – 37. As already described above, the values for module B are very low compared to the ones in module A and C. Module C shows the highest N_2O-N/ NH_4-$N_{conv\ ratio}$ with 1.3%, followed by 0.7% for module A. The lowest value shows module B with 0.2% N_2O-N/ NH_4-N_{conv}, while it needs to be said that the values regarding N_2O emissions of module be need to be doubted for operation phase 1 and 2. A total N_2O emission of the plant ca not be given for operation phase 1 and 2 since no reliable data regarding process air are available.
The ratio of the dissolved N_2O in the effluent from the modules and the emitted N_2O from the modules was calculated. For process days 33 – 37, the $N_2O_{dissolved}/N_2O_{emitted}$ was at 40±2.

Table 9 N_2O emission over modules and process air off for process day 61 - 66

	N_2O-N [g/d/m²]	N_2O-N/ NH_4-N_{conv} [%]
Module A	0.05 ±0.01	0.5 ±0.001
Module C	0.07 ±0.02	0.7 ±0.002

Table 9 shows the same as Table 8, but for process time 61 – 66. No results for module B are shown since the N_2O concentration was zero for this process time. With values between 0.5 and 0.7% N_2O-N/ NH_4-N_{conv}, the results are similar to the ones for process time 33 – 37 (Table 8).
The $N_2O_{dissolved}/N_2O_{emitted}$ ratio was at 105±10.

Table 10 N_2O emission over modules and process air off for process day 80 - 84

	N_2O-N [g/d/m²]	N_2O-N/ NH_4-N_{conv} [%]
Module A	0.05 ±0.01	3.9 ±1.4
Module B	0.1 ±0.01	2.1 ±0.1
Module C	0.09 ±0.0003	1.9 ±0.5
Process air	0.06 ±0.004	1.5 ±0.1

Table 10Table 11 shows the emission of the N_2O for process time 80 – 84. A process air in rate of 1L/h was set at this process time and therefore used for calculation. With values between 1.9 and 3.9% N_2O-N/ NH_4-N_{conv} the values vary significantly from the results shown in Table 8 and Table 9. A reason for the high value in module A is, that the module was blocked at process day 80 and therefore showed a NH_4-N removal rate of 1.7g/d/m², compared to 4.7 g/d/m² for module B or 5.5g/d/m² for module C (Table 4). This correlation can be seen in the values that are normalized on the membrane surface. It can be seen, that the N_2O emission in module A is with 0.05g/d/m² the lowest of all three modules, while the N_2O-N/ NH_4-N_{conv} is the highest of all three modules.
The emission by the process air was with 1.5% N_2O-N/ NH_4-N_{conv} lower than for all of the three modules, while the emission normalized on the membrane surface lies in between the values from the modules.
The total N_2O emission of the plant was 4.1%N_2O-N/ NH_4-N_{conv} for these process days.
The ratio of $N_2O_{dissolved}/N_2O_{emitted}$ was 49±9.

Table 11 N_2O-N emissions over modules and process air off for process day 94 - 98

	N_2O-N [g/d/m²]	N_2O-N/ NH_4-N_{conv} [%]
Module A	0.07 ±0.02	0.6 ±0.2
Module B	0.14 ±0.01	1.4 ±0.2
Module C	0.04 ±0.06	0.4 ±0.5
Process air	0.32 ±0.05	0.94 ±0.11

Table 11 shows the same as Table 10, but for process time 94 – 98. With values between 0.4 and 1.4% N_2O-N/ NH_4-N_{conv}, all values decreased significantly compared to the values from process time 80 – 84. Even though the process air was set from 1L/d to 2.1L/d, the ratio of N_2O-N/ NH_4-N_{conv} decreased. This can be explained with the higher NH_4-N removal rate in operation phase 4 compared to operation phase 3. The value for the N_2O-N emission normalized on the surface are increased almost by factor 6 from operation phase 3 to 4. Also the amount of N_2O emitted from the process air increased significantly. Additional, the value of N_2O emission from process air is higher than for all three modules combined.
The high standard derivation in module C is due to an outlier. The N_2O-N emission with cutting out this outlier is at 0.013±0.009g/d/m² or 0.11%±0.07%N_2O-$N_{removed}$/NH_4N-N.
The total N_2O emission of the plant was 1.7%N_2O-N/NH_4-N_{conv} for the balance calculated for operation phase 4.
The ratio of the $N_2O_{dissolved}$/$N_2O_{emitted}$ was at 93±2.

5 Discussion and conclusion

The fast build up of the biofilm was the main goal of the first operation phase. It took 45 days to build up a biofilm that could handle undiluted SDE, with a NH_4-N loading of 9gNH_4-N/m²/d. This means, that the NH_4-N loading rate can be increased by 0.29g/d/m² at the startup phase of the biofilm. At process day 61, the DO inside the bulk liquid was zero for the first time in all three modules and did not rise (except at blockings etc.) for the rest of the process time, therefore it can be said, that a good working biofilm was build up at that process time. Since the treatment of SDE with MABR was investigated for the first time in this thesis, no comparison regarding the biofilm build up can be given. Anyway, Cote et al., (2015) used municipal wastewater in a pilot-scale MABR and it took 40 days until it was said, that the biofilm was build up, while no specific criteria for the build up of the biofilm is given in the publication.

The ammonium removal rate constantly increased over the process time until it reached the maximum of 16.2 gNH_4-N/m²/d at process day 74, right before the leakage of process air at NV1 was detected. After the process air flow was set to 2.1L/h, the NH_4-N removal rate was at 12.6 gNH_4-N/m²/d which was the maximum of operation phase 4. Most likely, this was not the maximum removal rate possible for this setting. It can be assumed, that higher removal rate would have been possible by increasing the NH_4-N loading in the feed with the same strategy that was used for the earlier process time. Figure 21 supports this assumption, since OTE is at higher values for operation phase 3 than for operation phase 4. This means, that not the maximum of oxygen was transferred in operation phase 4 and therefore, an increase of the NH_4-N removal rate would have been possible. Further, higher removal rate can be seen in operation phase 2, while the process air in flow rate was most likely higher than in operation phase 4. Further tests should verify this assumption.
Achieving a high ammonium removal rate was one of the main goals of this study. A 50% ratio of NH_4-N_{conv} /NH_4-N_{feed} was achieved for operation phase 2, 3 and 4. In operation phase 1, the NH_4-N_{conv} /NH_4-N_{feed} conversion rate was at 75%. Additionally, an NH_4-N removal rate of 12.6 gNH_4-N/m²/d at a process air flow rate of 2.1L/h was achieved. As said earlier, the pH decreases due to the conversion of ammonium, therefore, a conversion rate above around 60% is not possible without adding dye to prevent inhibition of AOB due to low pH value. Cote et al., (2015) reported a maximum of the NH_4-N removal rate around 3gNH_4-N/d/m² using municipal wastewater. Another study (Brindl, et at., 1998). regarding treating synthetic wastewater (80mgNH_4/L) with MABR reported a specific nitritation rate of 5.4gNH_4-N/m²/d, while the ammonium concentration in the feed was at 80mgN/L, so significantly lower than in this thesis. An MABR consisting of silicone tubes was used for treating synthetic wastewater that contained 118 – 707mg$(NH_4)_2SO_4$/L. The maximum removal rate was 4.2gN/m²/d. This result was achieved with a N- loading rate of 8gN/m²/d in the feed (Hsieh, et al., 2001).
SDE has a very low C/N ratio, therefore it can be assumed, that a high number of nitrifying bacteria is in the biofilm. Through that, the high NH_4-N removal rate that was achieved can be explained, still it is suggested to perform a next generation DNA sequencing of the biofilm to find out about the bacteria.

The second goal of the study was to achieve partial nitrification. Except for process time 25 to 55, almost no nitrite accumulated in the system. Anthonisen (1972) reported, that inhibition of NOBs starts at 0.1-1mg/L of free ammonia. Anyway, Figure 14 shows, that free ammonia (FA) was around 1mg/L for process day 25 – 45 and even beyond 1mg/L until process day 80. Still, there was almost no nitrite in all three modules from process time 50 to 70. Anthonisen used flocculent sludge as well as no MABR technology, which could be a reason for the different results. Another reason could be,

that one of the characteristics of MABR is a high sludge age. Due to that, the bacteria can adapt to different process settings and do not get washed out even if they are inhibited. Therefore, it is much harder to get specific bacteria out of an MABR system. The structure of a Biofilm is in general more dense than flocculent sludge. This means that the surrounding liquid can penetrate flocculent sludge much easier while bacteria on the membrane side of the biofilm can not be reached easily by the liquid. Since Antonisen did not investigate SDE with MABR, the threshold can not be taken for granted and needs adaption to be valid for MABR technology. A second factor for inhibition of NOBs is free nitrous acid (FNA) (Zhou, 2011). The concentration of FNA and the concentration of NO_2^- are linked and can be calculated using Eq.2. Therefore, FNA is not a suitable parameter in this study to start the inhibition of NOBs, since the temperature is not adjustable and therefore constant at room temperature. Additionally, a low pH value, which would benefit FNA is not targeted. Anyway, FNA will contribute inhibiting NOBs once NO_2^- accumulated.

Summed up it can be said, that the threshold values of FA and FNA did not affect the NO_2^- accumulation in this thesis. Regarding Eq.3 which describes the correlation between FA, temperature, pH and NH_4 concentration, high pH supports a rise of the value and therefore inhibition of NOBs. On the other hand, low pH supports high values for FNA (Eq.2), while NO_2^- needs to be already inside the system. As an outlook, a strategy of high pH (7.3 – 8.0) can be tested, to check if accumulation happens. Another strategy could be to use a non constant aeration. When the aeration is reduced, the bacteria are oxygen limited and the nitritation rate will decrease. Therefore the pH, as well as the NH_4 concentration inside the modules will rise and support inhibition of NOBs by FA. When NO_2^- accumulated, aeration can be increased again, to bring oxygen inside the system to stop the oxygen limitation of the bacteria. Once the AOBs are not limited anymore, ammonium will be converted and the pH will decrease again which supports FNA. With this strategy, partial nitrification in MABR could be achieved.
A similar result could be achieved by varying the NH_4 loading in the feed. At high loading rates, NH_4 will accumulate and pH will increase and therefore FA will increase. After decreasing the NH_4 loading rate again, the pH will decrease and therefore inhibition of NOBs by FNA will be supported (under the condition that NO_2^- is already in the system). This strategy seems more promising than the one mentioned above.
Inhibition of AOBs should be avoided, therefore it should be considered, that it is said, that inhibition of AOBs starts at 40 – 200mgNH_3/L or 0.02 to 0.1mgHNO_3/L (Nowak, 1996). It should be noted, that the values for FA (Figure 14) and FNA (Figure 16) in this process are far from these thresholds. Again, these values must be doubted to be suitable for MABR, so further investigations regarding that topic should be performed to find out about suitable values for MABR and SDE.

Another key parameter for partial nitrification is the temperature. While the temperature was not controlled (and was therefore at room temperature), higher temperatures could benefit nitrite accumulation. Investigations with municipal wastewater in an inverse turbulent bed reactor showed, that at 35°C and an N loading rate between 1.92 and 2.88gN/$L_{reactor}$/d, high amounts of NO_2^- accumulated in the system, while the ammonium removal rate was between 68 and 100%. Also, 50% partial nitrification was achieved (Bougard et al., 2006). Another investigation with synthetic wastewater achieved 92% partial nitrification by using MABR technology. Like above, the temperature was adjusted to 35°C (Gong et al., 2007). Investigations at the WWTP from which the SDE was taken from showed, that the effluent from the centrifuge has a temperature of 25 – 27°C, therefore treating SDE at higher temperature than in this thesis can be performed easily and is

suitable for a scale up.
Both strategies (varying the pH with different NH_4 loading rate of the feed or the aeration and increasing the temperature) are promising to achieve partial nitrification in MABR.

The calculation of the oxygen balance showed better balance quality by using the process air in flow rate (0.9 ±0.1), therefore the discussion is based on these values. On process day 75, the leakage was fixed and the process air in flow set to 1L/h. At process day 76, the OTE was at 0.69, which was the maximum for the process. It then constantly decreased to 0.25 at process day 83. On process day 76 the NH_4-N removal rate was between 9.5 and 8.7mgNH_4-N/m²/d, while it decreased to 5.6 to 4.2gNH_4-N/m²/d at process day 83 (Figure 17). Also, the NH_4-N loading rate in the feed was decreased from 20.7g NH_4-N/m²/d at process day 76 to 9.3g NH_4-N/m²/d at process day 83 (Figure 10). So both, the NH_4-N removal rate decreased and the NH_4-N loading rate in the feed was reduced in operation phase 3, to make sure that the pH does not reach values above 7.3. This lead to a decrease of the OTR from 5.8g/d at process day 76 to 2.0g/d at process day 83 (Figure 21). Since the process air in flow rate was constant at 1L/h for operation phase 3, the OTE decreased constantly until the end of operation phase 3, due the reduced oxygen demand of the bacteria. At the end of operation phase 3 and the beginning of operation phase 4, where the process air in flow was set from 1L/d to 2.1L/d, the NH_4-N loading rate in the feed was increased to 19gNH_4-N/m²/d at process day 89. On process day 91, the NH_4-N loading rate in the feed was at 21gNH_4-N/m²/d, while the NH_4-N removal rate was at 12.8gNH_4-N/m²/d. The OTR increased to values around 3gO_2/d for operation phase 4, while OTE reached with 0.18 and 0.17 the minimum values for the process. The OTR increases due to increasing oxygen demand of the bacteria, caused by the higher NH_4-N loading rate in the feed and NH_4-N removing rate. Still, the high process air in flow rate caused a low OTE.
Since crucial parameters were changed in operation phase 3 (NH_4-N loading rate was reduced and the process air was set to 1L/d), the representativeness for the full process of the OTE and OTR values must be confirmed in the further operation of the MABR. Anyway, other investigations showed that using similar technology but different wastewater, a maximum OTE of 0.5 – 0.55 was achieved (Cote, 2015).
Investigations regarding the efficiency of aeration systems showed, that for a plant for nitrification with 6 meter depth shows OTE between 0.48 – 0.52. It needs to be considered, that these values are for clean water, therefore the α value (for activated sludge 0.5 – 0.65) needs to be taken into account. So an OTE for nitrification of activated sludge shows an OTE of 0.22 – 0.34 (DWA, 2012).
Regarding operation phase 4, the OTE was at 0.17 which was the minimum for the operation phase 3 and 4 and overall a low value. This indicates again, that the plant was not at its maximum performance with the set process air in flow of 2.1L/h and the NH_4-N loading rate in the feed could have been further increased.
The MABR system showed a maximum OTE of 0.69, which is higher than given values from pressure aeration systems for activated sludge (0.22 – 0.34) and MABR technology for treating activated sludge (0.5 – 0.55). Further investigation should be performed to gain more reliable data regarding OTE, anyway with the data available it can be said, that MABR for treating SDE seems to be a promising technology regarding energy efficiency for aeration.

The third main topic of this thesis was to quantify the N_2O emissions. The N_2O emission caused by mixing and scouring air from each module, normalized on the NH_4 removal rate from the modules in operation phase 1 and 2 did not reach, for one exception, values above 1% (Table 8, Table 9). Significantly higher values were reached in operation phase 3 (Table 10). The N_2O emission caused by

the mixing and scouring from each module, normalized on the NH_4-N removal rate reached values between 1.9 and 3.9%.. The reasons for the low NH4-N removal rate in operation phase 3 is already discussed above. Still the N_2O emission normalized on the membrane surface showed similar values for operation phase 3 as for operation phase 4 (Table 10, Table 11), which is surprising. As said above, main parameters have been changed in operation phase 3 which makes it hard to find the reason for the behavior. One reason could be the change of the NH_4-N loading rate in the feed during operation phase 3. Further the decrease of the NH_4-N removal rate in operation phase 3 indicates an oxygen limitation, which could lead to an increase of the N_2O emissions. Additionally, NO_2^- accumulation happened in operation phase 3, which again could have increased the N_2O emissions. Values from 0.4%N_2O-N/NH_4-$N_{removed}$ to 1.4N_2O-N/NH_4-$N_{removed}$ were seen in operation phase 4 for the emission caused by mixing air from the modules.
Process air showed for the ratio of N_2O-N/NH_4-N_{conv} values of 1.5% for operation phase 3 and 0.9% for operation phase 4. Both of these values lie between the emission from the headspace of the modules. Looking at the values of N_2O-N emission normalized to the membrane surface, it can be seen that for operation phase 3, the value (0.06gN_2O/d/m²) lies again in between the values from the emission from the headspace of the modules, while in operation phase 4, the emission from the process air was higher than for all three modules combined.
Overall it can't be said if the emission from the modules or the emission in the process air contribute the major part to the total N_2O emissions. Table 11 indicates, that process air contributes the major part, while Table 10 does not. A real conclusion can not be given at this place, since too little data is available. Anyway, it can be assumed, that the N_2O loading rate in the process air is higher than for the modules, since the conversion of NH_4, where N_2O is a byproduct takes place mostly in the biofilm. Therefore, a high N_2O concentration can be assumed near the membrane surface, which supports diffusion into the membrane chords. Still, this assumption needs to be validated by further experiments.
An emission factor of 0.8%N_2O/N-oxidized was achieved with partial nitritation coupled with anammox of reject wastewater in a 1-stage SBR in full scale (Joss et al., 2009). Another investigation with a lab scale SBR also showed an emission factor of 0.8%N_2O/N-oxidized (Rodriguez Caballero et al., 2013). An investigation regarding partial nitritation of reject wastewater with anammox in a 1-stage full scale treatment plant showed an emission factor of 2.5%N_2O/N-oxidized (Kampschreur et al., 2009). Also, Castro-Barros (2015) investigated partial nitritation of reject wastewater with anammox in a 1-stage WWTP at full scale. The emission facto was at 4.0%N_2O/N-oxidized. For partial nitritation coupled with anammox of anaerobic digested industrial wastewater in a full scale 2-stage wastewater treatment plant showed emissions from the nitritation reactor of 8.1 – 11.2%N-N_2O/N-oxidized (Desloover et al., 2011). Another thesis investigated the N_2O emission of a 2- stage full scale wastewater treatment plant treating reject wastewater with partial nitrification and anammox. The nitritation reactor showed an emission of 3.4%N-N_2O/N-oxidized (Kampschreur et al., 2008)
Except for operation phase 3, the MABR technology tested in this thesis can compete with the emission factors of 1-stage treatment plants. For the value given from the investigations of 2-stage wastewater treatment plants, the N_2O emission from the MABR technology in this thesis is significantly lower.

The emission of N_2O from the modules is measured in the headspace of the modules. The volume of this headspace is approximately 0.36L/module. An air flow rate of 0.04L/mixing were used for mixing, therefore it takes about 10 mixing circles to replace the air in the headspace. Since mixing was performed every two minutes, it took 20 minutes to replace the air in the headspace of the module

with mixing air. The air flow rate for scouring is between 1.35 and 1.73L/scouring, therefore, the air inside the headspace is replaced about 4 times by one scouring circle. The measurements of the N_2O concentration in the headspace showed, that the N_2O content does not change drastically after one mixing circle. It can be assumed, that N_2O is diffusing from the liquid phase into the gas phase during the time no mixing takes place. Further it can be assumed, that mixing air strips out N_2O, but also "dilutes" the amount of N_2O in the head space. Since the N_2O concentration in the headspace does not change drastically after each mixing cycle it can be assumed, that the effect of stripping N_2O by mixing air, dilution by mixing air and diffusion of N_2O from the liquid phase into the gas phase are compensating. Anyway, investigations during scouring cycles showed, that the N_2O concentration in the headspace of the modules decreased during the scouring. Since scouring is performed with a much higher air flow rate, the stripping effect should be increased, while on the other hand also the dilution effect should increase. The fact, that the N_2O content decreased during a scouring circle speaks for a high impact on the emission of N_2O by the diffusion effect mentioned above. Anyway, these are all hypothesis and need further investigations to be verified.
Scouring is used to remove surplus biofilm from the membranes, out of the gathered experience with treating SDE with MABR it can be said that the scouring frequency could be reduced to one time per day. Further, the mixing cycles could be reduced from 10 seconds on/110 seconds off to 10seconds on/230seconds off. Theoretically, the emissions can be reduced by 50%, while it should be said, that higher concentration of N_2O in the bulk could result from this reduction of the airflow. As a consequence, more N_2O could be stripped out in each mixing circle, which would increase the N_2O content in the headspace. Anyway, this approach should be tested in further experiments.
Also, the N_2O inside the process air is in a defined air flow which can be handled easily. Table 11 showed, that the emission over process air contributes more than 50% of the total N_2O emission of the plant, while Table 10 did not validate this as a general behavior of the MABR system. Further treatment to remove the N_2O and therefore prevent emission could be applied for process air, for example an adsorption over zeolites (Centi et al., 2000).
The idea is to bring the effluent after treatment with MABR into the anoxic part of a wastewater treatment plant to perform denitrification. Therefore, the N_2O inside the bulk liquid (Figure 24) will not be stripped out due to aeration but further converted to N_2. Calculations regarding the $N_2O_{dissolved}/N_2O_{emitted}$ ratio showed, that 49 – 105 times more N_2O is dissolved in the effluent compared to what is emitted by the modules. This shows the potential of reduction of N_2O emissions that can be achieved with the method described above.

Overall it can be said, that treating SDE with MABR is a suitable technology. While partial nitrification could not have been achieved over almost the full process time, there are still different strategies that can be applied to achieve partial nitrification. With a high NH_4-N removal rate, potentially high OTE and low N_2O emissions normalized on the NH_4-N removal rate, it is an efficient technology regarding energy efficiency and emission of greenhouse gases and therefore a promising technology for the future.

6 References

Adams, N., Hong, Y., Ireland, J., Koops, G.H. and Côté, P. (2014) A New Membrane-Aerated Biofilm Reactor (MABR) for Low Energy Treatment of Municipal Sewage. Singapore International Water Week, (SIWW), Singa-pore

Anthonisen, A. C., et al. "Inhibition of nitrification by ammonia and nitrous acid." Journal (Water Pollution Control Federation) (1976): 835-852.

Appels, Lise, et al. "Principles and potential of the anaerobic digestion of waste-activated sludge." Progress in energy and combustion science 34.6 (2008): 755-781.

Bae, Wookeun, et al. "Optimal operational factors for nitrite accumulation in batch reactors." Biodegradation 12.5 (2001): 359-366.

Blackburne, Richard, Zhiguo Yuan, and Jürg Keller. "Partial nitrification to nitrite using low dissolved oxygen concentration as the main selection factor." Biodegradation 19.2 (2008): 303-312.

Bougard, D., et al. "Nitrification of a high-strength wastewater in an inverse turbulent bed reactor: effect of temperature on nitrite accumulation." Process Biochemistry 41.1 (2006): 106-113.

Brindle, Keith, Tom Stephenson, and Michael J. Semmens. "Nitrification and oxygen utilisation in a membrane aeration bioreactor." Journal of Membrane Science 144.1 (1998): 197-209.

Castro-Barros, Celia Maria, et al. "Effect of aeration regime on N 2 O emission from partial nitritation-anammox in a full-scale granular sludge reactor." water research 68 (2015): 793-803.

Centi, G., et al. "Removal of N2O from industrial gaseous streams by selective adsorption over metal-exchanged zeolites." Industrial & engineering chemistry research 39.1 (2000): 131-137.

Côté, Pierre, et al. "A New Membrane-Aerated Biofilm Reactor for Low Energy Wastewater Treatment: Pilot Results." Proceedings of the Water Environment Federation 2015.13 (2015): 4226-4239.

Chen, Xueming, et al. "A new approach to simultaneous ammonium and dissolved methane removal from anaerobic digestion liquor: A model-based investigation of feasibility." Water research 85 (2015): 295-303.

Desloover, Joachim, et al. "Floc-based sequential partial nitritation and anammox at full scale with contrasting N 2 O emissions." Water Research 45.9 (2011): 2811-2821.

DWA 2012
DWA-M 229 (Entwurf 2012): “System zur Belüftung und Durchmischung von Belebungsanlagen“

Flechard, C. R., et al. "Effects of climate and management intensity on nitrous oxide emissions in grassland systems across Europe." Agriculture, Ecosystems & Environment 121.1 (2007): 135-152.

Ge, Shijian, et al. "Detection of nitrifiers and evaluation of partial nitrification for wastewater treatment: a review." Chemosphere 140 (2015): 85-98.

Gong, Zheng, et al. "Feasibility of a membrane-aerated biofilm reactor to achieve single-stage autotrophic nitrogen removal based on Anammox." Chemosphere 69.5 (2007): 776-784.

Hellinga, C., et al. "The SHARON process: an innovative method for nitrogen removal from ammonium-rich waste water." Water science and technology 37.9 (1998): 135-142.

Hsieh, Yuan-Lynn, Szu-Kung Tseng, and Yu-Jie Chang. "Nitrification using polyvinyl alcohol-immobilized nitrifying biofilm on an O2-enriching membrane." Biotechnology Letters 24.4 (2002): 315-319.

IPCC (2007). IPCC – Intergovernmental Panel on Climate Change. The Physical Science Basis, contribution to the fourth Assessment Report (AR4), 2007, http://www.climatechange2013.org/

Joss, Adriano, et al. "Full-scale nitrogen removal from digester liquid with partial nitritation and anammox in one SBR." Environmental Science & Technology 43.14 (2009): 5301-5306.

Kampschreur, Marlies J., et al. "Dynamics of nitric oxide and nitrous oxide emission during full-scale reject water treatment." Water Research 42.3 (2008): 812-826.

Kampschreur, Marlies J., et al. "Nitrous oxide emission during wastewater treatment." Water research 43.17 (2009): 4093-4103.

Kampschreur, M. J., et al. "Emission of nitrous oxide and nitric oxide from a full-scale single-stage nitritation-anammox reactor." Water Science and Technology 60.12 (2009): 3211-3217.

Krampe J., Parravicini V., Baumgartner T., Svardal K. (2016)
Die Kläranlage als Baustein zur Energiewende?
Oral presentation at 88. Darmstädter Seminar – Abwassertechnik, 25/05/16, Technische Universität Darmstadt, Institut IWAR (Germany)

Lackner, Susanne, et al. "Nitritation performance in membrane-aerated biofilm reactors differs from conventional biofilm systems." Water research 44.20 (2010): 6073-6084.

Martin, Kelly J., and Robert Nerenberg. "The membrane biofilm reactor (MBfR) for water and wastewater treatment: principles, applications, and recent developments." Bioresource technology 122 (2012): 83-94.

Meyer, S. S., and P. A. Wilderer. "Reject water: Treating of process water in large wastewater treatment plants in Germany—A case study." Journal of Environmental Science and Health, Part A 39.7 (2004): 1645-1654.

National Institute of Standards and Technologies
URL: http://webbook.nist.gov/cgi/cbook.cgi?ID=C10024972&Mask=10 (07.05.2017, 15:55)

Nowak, Otto.” Nitrifikation im Belebungsverfahren bei maßgebendem Industrieabwassereinfluß.“ Inst. für Wassergüte u. Abfallwirtschaft, TU Wien, 1996.

Parravicini et al., „ReLaKo Reduktionspotential bei den Lachgas-Emissionen aus Kläranlagen durch optimierung des Betriebs“ (2015)

Rodríguez-Caballero, Adrián, and M. Pijuan. "N 2 O and NO emissions from a partial nitrification sequencing batch reactor: exploring dynamics, sources and minimization mechanisms." Water research 47.9 (2013): 3131-3140.

Tallec, Gaëlle, et al. "Nitrous oxide emissions from secondary activated sludge in nitrifying conditions of urban wastewater treatment plants: effect of oxygenation level." Water research 40.15 (2006): 2972-2980.

European Comission: “Annual European Union greenhouse gas inventory 1990-2014 and inventory report” (2016): 682-683

Wang, Qilin, et al. "Heterotrophic denitrification plays an important role in N 2 O production from nitritation reactors treating anaerobic sludge digestion liquor." water research 62 (2014): 202-210.

Yoon, Seong-Hoon. Membrane bioreactor processes: Principles and applications. CRC Press, 2015.

Zheng, Hong, Keisuke Hanaki, and Tomonori Matsuo. "Production of nitrous oxide gas during nitrification of wastewater." Water Science and Technology 30.6 (1994): 133-141.

Zheng, Maosheng, et al. "Minimization of nitrous oxide emission in a pilot-scale oxidation ditch: Generation, spatial variation and microbial interpretation." Bioresource technology 179 (2015): 510-517.

Zhou, Yan, et al. "Free nitrous acid (FNA) inhibition on denitrifying poly-phosphate accumulating organisms (DPAOs)." Applied microbiology and biotechnology 88.1 (2010): 359-369.

7 Figures

Figure 1
Thomas Baumgartner, TU Wien

Figure 4
Kampschreur, Marlies J., et al. "Nitrous oxide emission during wastewater treatment." Water research 43.17 (2009): 4093-4103.

Figure 7
Zebo Long, GE Waters